2016

COMPETITION VEHICLE BASED INTAKE MANIFOLD DESIGN

Joshua N. Matiash
Michigan Technological University, jnmatias@mtu.edu

COMPETITION VEHICLE BASED INTAKE MANIFOLD DESIGN

By

Joshua N. Matiash

A REPORT

Submitted in partial fulfillment of the requirements for the degree of

MASTER OF SCIENCE

In Mechanical Engineering

MICHIGAN TECHNOLOGICAL UNIVERSITY

2016

This report has been approved in partial fulfillment of the requirements for the Degree of MASTER OF SCIENCE in Mechanical Engineering.

Department of Mechanical Engineering – Engineering Mechanics

Report Advisor: *Dr. Scott A. Miers*

Committee Member: *Dr. James DeClerck*

Committee Member: *Dr. David D. Wanless*

Department Chair: *Dr. William W. Predebon*

Contents

Abstract

A competitive vehicle in Formula SAE needs to be easy for unskilled drivers to extract the maximum performance from. This requires a predictable and manageable torque curve. This report details the development of an intake manifold for a Formula SAE car from a vehicle-based approach to produce this manageable and predictable torque. The current vehicle was instrumented and driven on a representative track to determine the usage of available torque. Based on these findings an ideal torque curve was chosen that favored increased torque at upper engine speed ranges and decreased torque at lower engine speed ranges.

A 1-D engine cycle simulation model was developed and calibrated from intake, cylinder, and exhaust pressures measured on a dynamometer. The combustion model used the Wiebe function to model the burn rate and determine the simulated cylinder pressure. A design of experiments was performed with the calibrated 1-D model to find the optimized intake manifold geometry. Primary runner length and inlet diameter as well plenum volume were investigated and sized to produce as close to the ideal torque curve as possible. Based on this geometry a 3-D CAD model was developed and 3-D printed for use on the engine.

The fuel delivery and ignition timing of the engine with the 3-D printed intake manifold were tuned on a dynamometer and the torque curve produced was found to be similar to the predicted torque curve at the upper engine speed range but deviate at the mid-range. An on-track vehicle comparison of the new intake manifold to the old intake manifold was attempted but not completed due to cracking of the new intake manifold under vacuum on the vehicle.

Chapter 1

Introduction

1.1 Background

1.1.1 FSAE Competition

In the Formula SAE (FSAE) collegiate design competition, engineering students from across the globe design and build open-wheel race cars to compete against each other. The drivers for MTU's FSAE team are members of the team, and engineering students, not professional race drivers. For this reason, it is important to have an easy to drive and predictable vehicle. The torque delivery of the vehicle needs to be manageable and predictable for the driver to consistently drive at the limit. While a predictable and controllable vehicle is important, it is also important to have enough power for the vehicle to perform competitively. This means the torque curve is crucial to the overall performance of both the driver and vehicle.

The FSAE rules put many limitations on the engine, including:

- Four Stroke, Reciprocating Piston Type
- Maximum Displacement of 710 cc
- All Intake Air Must Pass Through a Circular 20 mm Diameter Restrictor
- Throttle Body Must Be Before the Restrictor

Due to the limitations put on the vehicle by the rules, the budget limitations of the MTU FSAE team, and the limited high-performance driving experience of the drivers, it is important for the vehicle to be as optimized as possible.

1.1.2 Intake Manifold Tuning

For a given engine displacement and technology, the amount of integrated torque, or "area under the curve" is largely fixed. The maximum torque generated at a given engine speeds is a product of the air and fuel burned in the cylinder. In a spark-ignited (SI) engine, air leads and fuel follows, meaning the output is controlled by controlling the airflow into the engine. Increasing the maximum airflow at a given engine speed, with an appropriate increase in fuel delivered, will increase the torque output at that speed. The amount of airflow into the cylinder at a given engine speed can be maximized by tuning the intake manifold to have ideal Helmholtz resonance characteristics [1]. This tuning is only ideal for certain engine speeds, and can negatively affect airflow at other engine speeds. Heywood [2] shows the effects of intake runner length on the volumetric efficiency (VE) of an engine across its speed range, which can be seen in Figure 1.1.

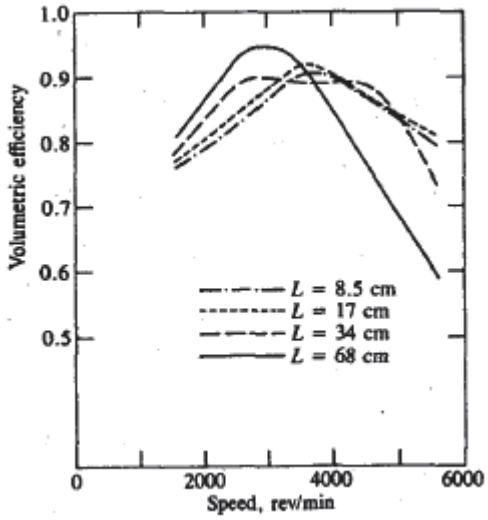

Figure 1.1: Volumetric efficiency for different intake runner lengths [2].

In Figure 1.1 notice that the longer runners increased VE at lower engine speeds, but decreased VE at higher engine speeds, and the short runners had the opposite effect. Therefore, the torque curve can be tuned by careful selection of intake manifold geometry.

Torque can be increased without sacrifice by adding "technology" such as forced induction, variable valve timing, active intake manifolds, etc., but at the cost of increased mass and cost. So

to improve the performance of a FSAE race car without adding mass and cost, the torque needs to be generated efficiently, without wasting torque at engine speeds where it will be unusable due to wheel spin.

1.2 Hypothesis

Tuning the intake manifold geometry so the engine delivers an optimized amount of torque throughout the engine speed range will improve the overall vehicle performance in the form of lower lap times. Tuning the torque curve with the intake manifold so there is no "wasted" or unusable torque will mean the engine is working at its maximum effectiveness for the vehicle. The optimized torque curve will improve drivability because the vehicle will be less likely to break traction under power. Improving drivability can result in more consistent lap times with less driver fatigue, and more driver confidence. The improved confidence allows the driver to push the vehicle to the limit, extracting the maximum possible performance.

Chapter 2

Procedure

2.1 On-Track Torque Usage Investigation

To optimize the intake manifold geometry for the lowest lap times, the target torque curve first had to be determined. This was accomplished by first determining how the torque previously available (old intake design) was used by the vehicle. With fixed atmospheric conditions, the torque an engine produces at any time depends only on the manifold absolute pressure (MAP) and engine speed, assuming consistent fueling. For example, running the same engine, with the same intake, exhaust, and fuel/spark calibration, on a dynamometer versus in a vehicle. So the torque the engine develops on-track can be determined by recording the MAP and engine speed then recording the torque on an engine dynamometer at the same MAP and engine speed points.

Since the FSAE competition only takes place once a year in May, the actual endurance track could not be driven so an accurate representation had to be developed to fit in the space available. A track was designed based on the FSAE track, featuring approximately 1/3 of the features, but with straights and a slalom the same length as the FSAE track. The overall track length was 1625’ (0.3 miles). Figure 2.1 shows the 2015 FSAE endurance track. Figure 2.2 shows the test track developed for the Houghton County Memorial Airport (CMX).

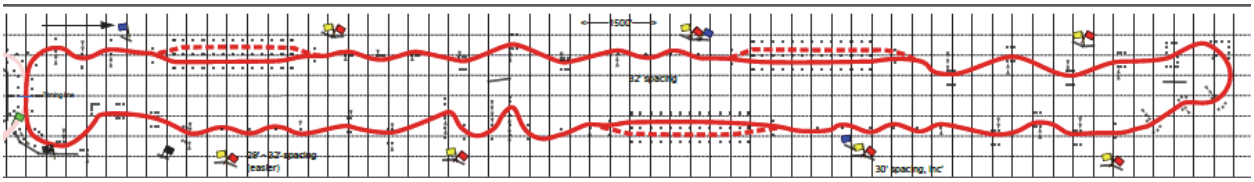

Figure 2.1: 2015 FSAE endurance track [3].

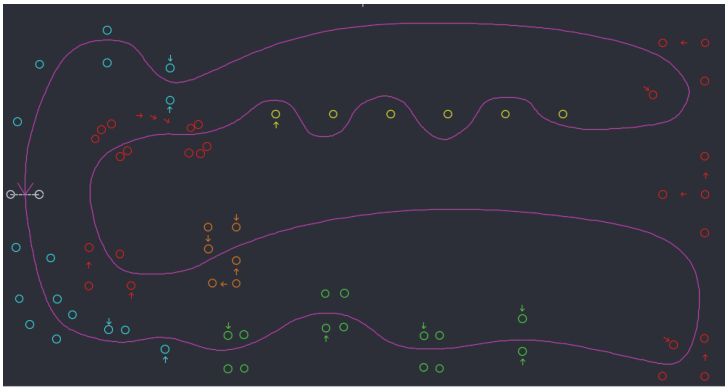

Figure 2.2: CMX test track based on 2015 FSAE endurance track.

The engine parameters (engine speed and MAP) were measured using a Performance Electronics (PE) ECU, which has built-in data acquisition (DAQ) capabilities. Vehicle position and engine speed were measured using an AIM EVO4 DAQ system with built-in GPS. This data was aligned based on engine speed so it would be possible to determine engine torque and power on the track, such as mid-corner, corner exit, and on straights.

The test vehicle, the F194, was a race-proven chassis, having competed in the 2015 FSAE competition with the Yamaha Genesis 80 two cylinder engine. No aspects of the chassis or drivetrain were changed during the test. To gain a broader understanding of the torque needs, multiple intake manifold/calibration combinations were developed, with the goal being to have several power levels for the vehicle. This included a 19 mm intake restrictor, 25 mm intake restrictor, and appropriate engine calibrations. Table 2.1 below provides a breakdown of the intake/calibration setups used.

Table 2.1: Intake restrictor/calibration setups used during F194 track testing.

Run Number	Intake Restrictor	Calibration
1	25mm	19mm Race Cal
2	25mm	25mm Cal
3	19mm	19mm Race Cal

Each combination was run for 3-5 laps around the test track, with the driver focused on being as fast as possible while still remaining consistent. To determine the torque and power used on track, the engine was run on the dynamometer at the same MAP and engine speed points. To accurately represent the vehicle, the exhaust system from the F194 was used on the dyno, with slight

modification so the exhaust could be routed to the building exhaust vents. The header was unmodified so the primary exhaust runners were the same as the vehicle. The only thing different from the test track driving was the atmospheric conditions, which though recorded at the test track, were not recorded in the dyno cell during testing. The track testing temperature was 17 °C, while the dyno cell was thermostatically controlled around room temperature, approximately 21 °C.

The engine was run with the setups seen above from 4,000 rpm to 12,500 rpm while sweeping the MAP (opening and closing the throttle) at 500 rpm increments. PE was once again used to record MAP and engine speed, including the exact same MAP sensors used on-track. Dynomax software was used to record engine speed and torque, and the engine speed data was used to align the two sets of data. The post processing and results are discussed in Chapter 3.1.

2.2 Engine Model Development

Once the target torque curve had been established, a reliable model of the engine was needed to find the intake design that would best meet the torque target. This was achieved by developing a 1-D engine simulation using GT-Power, and was calibrated based on intake, cylinder, and exhaust pressures measured on a dynamometer. To measure these pressures, the engine was instrumented with several special pressure transducers and a crankshaft encoder recorded with a combustion analysis system. The data was recorded and reviewed, then input into GT-Power and the combustion model was calibrated.

2.2.1 Engine Dynamometer Testing

2.2.1.1 Engine Instrumentation

To obtain high-speed intake, cylinder, and pressure measurements, an ACAP combustion analysis data acquisition system, made by DSP Technologies, was used. Table 2.2 summarizes the ACAP hardware.

Table 2.2: ACAP data acquisition hardware summary.

Model	Description
DSP Technologies Porta 416	12 Slot Chassis
4325	TRAQ Real Time Processor
5008	8192K Memory Module
4012A	TRAQ I System Controller
2860	4 Channel Timer/Digitizer
2904A	Spincoder Timer/Counter
1104CM	4 Channel Charge Amplifier
6001	CAMAC Microprocessor

The ACAP combustion analysis system required a high-speed encoder reading engine position. A 720 pulse per revolution encoder was selected so pressure measurements could be made at every ½ degree of crankshaft rotation. An Encoder Products (EPC) Model 121 was chosen. It is a non-contact encoder that is compatible with the engine's maximum angular velocity of 13,000 rpm. A data sheet on the EPC 121 can be found in Appendix A.

A mount was designed that pressed into a crankshaft bolt access hole on the ignition cover to rigidly mount the encoder on the engine. Figure 2.3 below shows the ignition cover of the engine that the mount was pressed into.

Figure 2.3: Yamaha Genesis 80 ignition cover, before the encoder mount was pressed in.

A drawing for the encoder mount can be found in Appendix A. The encoder attached to the crankshaft via an adapter shaft designed to replace the flywheel bolt. A drawing of the encoder adaptor shaft can be found in Appendix A. Figure 2.4 shows the mount and shaft on the engine, with the encoder mounted.

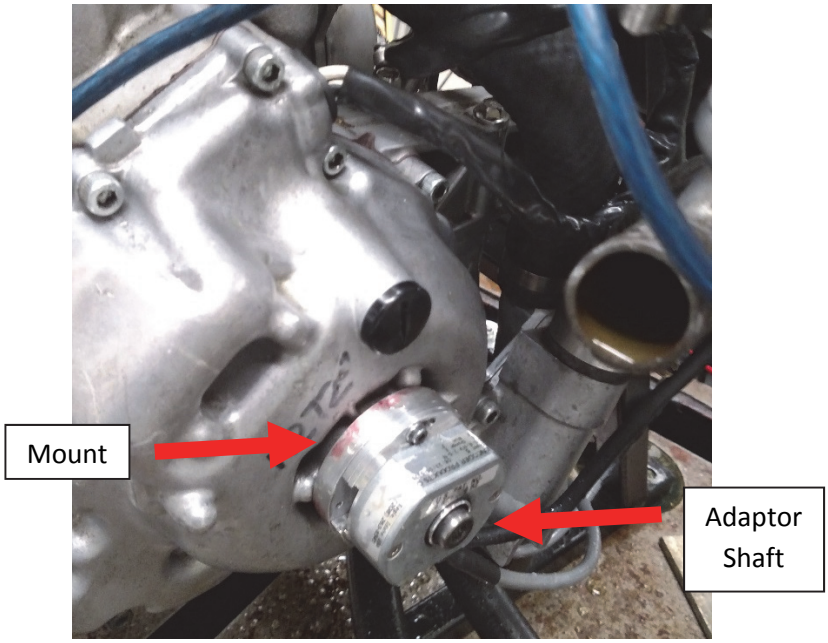

Figure 2.4: Engine with EPC 121 encoder mounted. Note the aluminum encoder mount and steel adaptor shaft.

Initially the adaptor shaft was machined with a 15 mm OD, and the encoder was specified with an ID of 15 mm. This clearance proved too tight and the force required to press the encoder onto the shaft resulted in a cracked encoder rotor which led to complete encoder failure. The adaptor shaft was machined down so the encoder could easily slide on and a new encoder was installed.

The encoder signal was fed into the ACAP system with BNC cables for the A pulse (720 pulses/revolution) and Z pulse (1 pulse/revolution). ACAP uses the A pulse to trigger the recording of the intake, cylinder, and exhaust pressures.

The new encoder worked with the ACAP system at engine speeds below 6,000 rpm but an encoder error occurred at greater engine speeds. An attempted solution was to use a thin rubber sheet as an isolator for the encoder body, but this allowed too much movement between the encoder body and rotor, which resulted in encoder failure. The final solution was to mount the encoder directly to

the mount, and retighten the mounting bolts and clamping bolt after every data collection run. There were no encoder errors below 11,500 rpm after this. Above this engine speed high-speed pressure data was not collected due to the encoder errors.

To measure pressure in the intake port a Kulite ETL-179X-190M piezoresistive pressure transducer was used. The cylinder head was machined to place the intake pressure transducer at the beginning of the intake port. The exhaust pressure was measured 25 mm after the exhaust port by welding a bung onto the header. This bung was drilled and tapped to accept the Kulite EWCTV-312M pressure transducer. A drawing of the Kulite ETL-179X-190M and EWCTV-312M can be found in Appendix A. The Kulite EWCTV-312M is a liquid-cooled transducer. A 20 gallon/hour garden water fountain pump was used to pump tap water from a half-full five gallon bucket through the sensor and back.

The cylinder was machined for a PCB 115A04 cylinder pressure transducer. Due to the tight packaging of the head, only cylinder 2 was instrumented. Figure 2.5 shows the instrumented engine with the intake, exhaust, and cylinder pressure transducers in place.

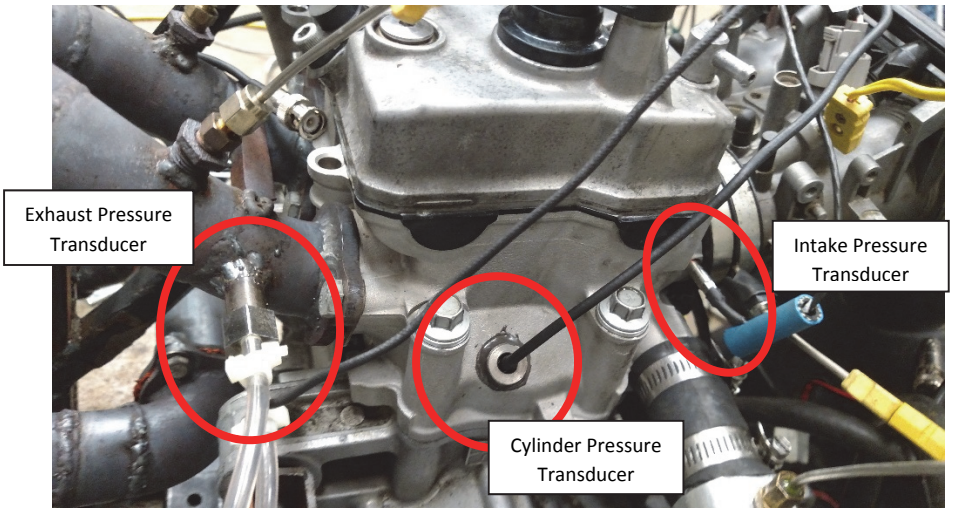

Figure 2.5: Instrumented Yamaha Genesis 80 cylinder head.

The signals from the three pressure transducers were fed into the ACAP system for high-speed acquisition. The high-speed pressure data was recorded for 300 cycles at each speed/load point. Table 2.3 provides a summary of the high-speed instrumentation.

Table 2.3: High-speed instrumentation summary.

Parameter	Device	Specifications
Cylinder Pressure	PCB 115A04 Pressure Transducer	Sensitivity: 211.7 pC/MPa
Intake Port Pressure	Kulite ETL-179X-190M Pressure Transducer	Range: 0-2 bar absolute
Exhaust Port Pressure	Kulite EWCTV-312M Pressure Transducer	Range: 0-3.5 bar absolute
Engine Crankshaft Position	Encoder Product Model 121	Resolution: 0.5 CAD

Other parameters of engine performance were monitored and recorded using L&S, such as torque, engine coolant temperature, engine oil temperature, intake air temperature, exhaust gas temperature (EGT), air/fuel ratio (AFR), engine speed, and fuel flow at 1 Hz. The low-speed data was collected at each speed/load point for the duration of the 300 cycles. Table 2.4 below provides a summary of the low-speed instrumentation.

Table 2.4: Low-speed instrumentation summary.

Parameter	Device
Torque	Land & Sea DYNOmite Dynamometer Strain Gauge
Engine Coolant Temperature	Type K Thermocouple
Engine Oil Temperature	Type K Thermocouple
Intake Air Temperature	Type K Thermocouple
Exhaust Gas Temperature	Type K Thermocouple
Air/Fuel Ratio	Innovate LC-1 Narrowband Oxygen Sensor
Engine Speed	Land & Sea Hall Effect Sensor
Fuel Flow	Re-Sol RS822-85 Fuel Flow Measurement System

These parameters along with the pressure data would be used to calibrate the combustion model in the GT-Power simulation, which is discussed in Chapter 3.2.

2.2.1.2 Dynamometer Setup/Testing

The engine was loaded using L&S DYNOmite 9” Toroid water brake. This water brake uses a strain gauge to measure torque. The strain gauge torque measurement was calibrated at 0 ft-lb and 25 ft-lb using an L&S calibrated weight. Figure 2.6 shows the engine on the bedplate with the water brake attached.

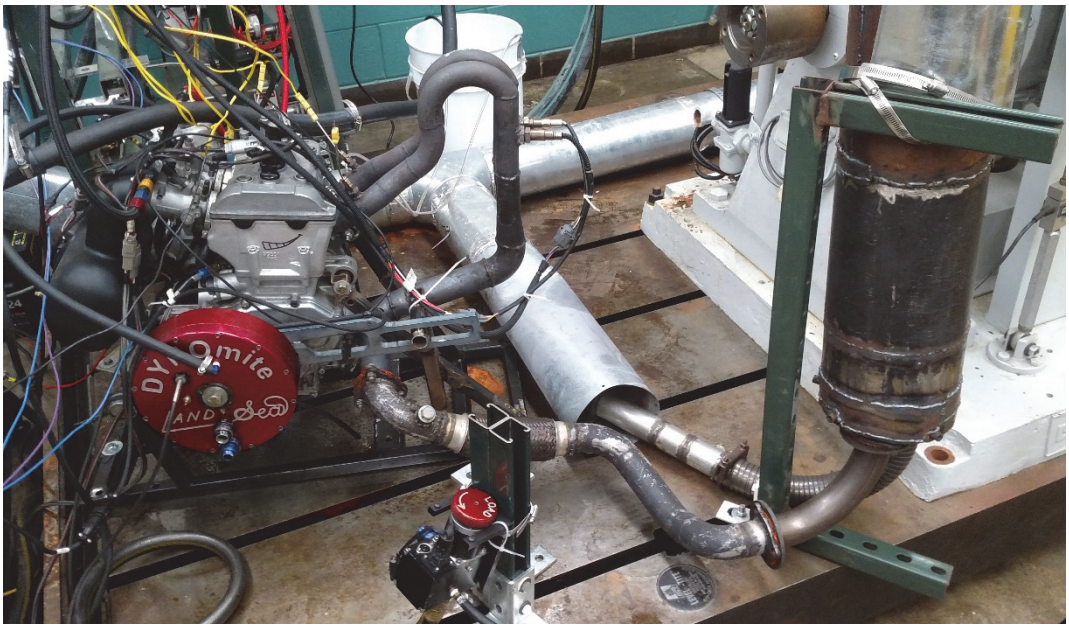

Figure 2.6: Engine setup on the test bed with the dynamometer attached.

The engine speed was electronically controlled using an L&S servo load valve, which regulates the amount of water going to the water brake using a PID controller to maintain a user-set engine speed. The throttle was electronically controlled using an L&S throttle servo. Data was collected with the engine at wide open throttle from 5,000 rpm to 11,500 rpm in 500 rpm increments.

2.2.2 GT-Power Model

The GT-Power model was developed based on an existing model the FSAE team had previously used. The model initially included accurate measurements of the cylinder geometry, camshaft profiles, camshaft centerlines, and cylinder head flow coefficients. These parameters can be found in Appendix B. The Gamma Technologies software GEM3D was used to accurately model the F194 intake manifold by importing a 3-D CAD file and converting it into flow components in GT-Power. Figure 2.7 shows the F194 model which was used to calibrate the combustion model based on the empirical data.

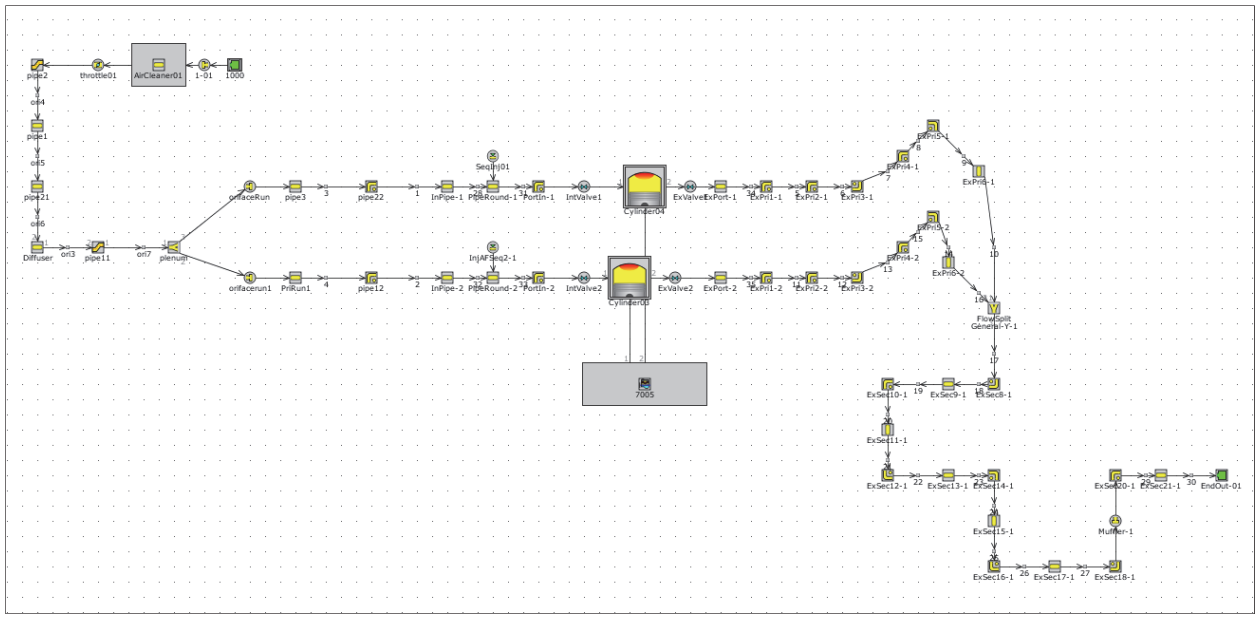

Figure 2.7: Initial GT-Power model of the F194 used to calibrate the combustion function

Initially a turbulent combustion model was attempted, but due to the lack of reliable and accurate information for many of the required model inputs regarding the engine and cylinder head, the Wiebe function was chosen. Some of the additional pieces of information included detailed piston combustion chamber, and port geometry, intake port tumble measurements, and flame speed. The Wiebe function, which generates an "S" curve that represents the burning of the air/fuel mixture, can be seen in Equation 2.1 below [4].

$$x_b = 1 - \exp\left[-a\left(\frac{\theta-\theta_0}{\Delta\theta}\right)^{m+1}\right] \quad \textbf{(2.1)}$$

Where x_b is the burned mass fraction, $\Delta\theta$ is the combustion duration in crank angle degrees, θ is the crankshaft position in crank angle degrees, and θ_0 is the start of combustion, typically the spark timing in an SI engine. The factors a and m are used to adjust the shape of the curve. GT-Power allows the user to input the 50% mass fraction burned location (CA50) in crank angle degrees, 10-90% mass fraction burn duration (D1090) in crank angle degrees and m to specify the Wiebe function used to model combustion.

The F194 model was calibrated by adjusting the flow components (intake and exhaust), CA50, and D1090 values until the AFR, fuel flow, VE, cylinder pressure, and torque output by GT-Power closely matched the empirical data. The results of this calibration can be seen in Chapter 3.3.

2.3 Intake Design

2.3.1 Intake Geometry Design of Experiments

With the GT-Power combustion model calibrated, a design of experiments (DOE) was run varying the intake primary runner length and inlet diameter of the F194 model. These parameters were chosen because the primary runner outlet diameter was fixed by the cylinder head intake port diameter, and the plenum volume would largely be dictated by the space available for the intake manifold in the vehicle. Table 2.5 shows the initial DOE values used.

Table 2.5: Initial intake geometry DOE parameters.

Intake Primary Runner Length [mm]	Intake Primary Runner Inlet Diameter [mm]
140	50
155	55
170	60

The initial DOE values were chosen because the torque curve target had a linear slope favoring high engine speed power, so the runners would likely need to be shorter than the stock length and the previous intake designs. Table 2.6 summarizes the geometry of previous intake manifolds.

Table 2.6: Previous MTU FSAE intake manifold geometry and stock Yamaha intake manifold geometry.

Dimension	Stock Yamaha	F194 (2014)	F315 (2015)
Runner Length [mm]	235	220	300
Runner Inlet Diameter [mm]	49	49	54
Runner Radius of Curvature [mm]	55	55	50

The torque results from the initial DOE were compared to the target torque line. Based on these results the intake geometry was then adjusted further to find the geometry that not only met the torque target but would also be manufacturable and fit in the design space available in the vehicle. The longest runner simulated was 240 mm while the shortest was 115 mm. The intake manifold had to attach to the cylinder head and fit between the engine block and firewall, which would necessitate a radius of curvature for the runners of no more than 60 mm. With these constraints in

mind further iterations of intake geometry were simulated and compared to the target torque. The final intake geometry and torque prediction can be found in Chapter 3.4.

2.3.2 CAD Model Development

Once the optimum intake manifold geometry was found a 3-D CAD model was developed using Siemens NX 10. The intake needed to incorporate provisions for the fuel injectors, fuel rail, MAP sensor, restrictor, intake-to-head mounting boots, and mounting tabs. The intake was to be 3-D printed by McLaren Engineering, who has printed five intake manifolds for the MTU FSAE team in the past. The printer used was a Statasys FDM 400mc printing Polycarbonate-ABS. The MTU FSAE team had previously performed a successful gasoline soak test with the material and incorporated the fuel injectors in printed manifolds, so a similar fuel injector mounting method was to be used, with the fuel injectors in the stock position. The final intake 3-D CAD model and final printed intake can be seen in Chapter 3.5.

2.4 Final Validation

Once the new intake was printed, the engine needed to be calibrated for use in the new MTU FSAE car, the F260. The fuel delivery for the engine with the new intake was calibrated on the dynamometer with a target AFR of 12.5:1 as this is the stock Yamaha calibration target. The ignition timing was calibrated for safe EGTs and knock avoidance. The calibration was finalized in-vehicle for drivability. Once the calibration was deemed acceptable the torque output was compared to the GT-Power prediction. The actual torque versus predicted torque comparison can be found in Chapter 3.6.

The final test of hypothesis was to drive the vehicle on-track with the old (F315) and new (F260) intake manifolds. The same course as shown in Figure 2.2 was setup at CMX. The track testing consisted of driving the vehicle with the different intake manifolds back-to-back, as shown by Table 2.6. Each test run would consist of four laps, with the final two laps timed using infrared timers.

Table 2.6: On-track intake manifold test order.

Intake Manifold	Driver
F315	A
F260	A
F315	B
F260	B
F260	A
F260	B
F315	A
F315	B

The goal of the final validation was to compare lap times of the old F315 intake and new F260 intake. The F194 intake originally used for testing does not fit on the new vehicle, the F260, so it cannot be compared on-track. The results of the on-track comparison can be found in Chapter 3.6.

Chapter 3

Results and Discussion

3.1 On-Track Torque Usage Findings

To determine the on-track torque from the track data, Matlab was used to create surface fits from the dynamometer data. Each surface relates MAP and engine speed to torque, and surfaces were generated in 1,000 rpm increments, from 4,000 rpm to 13,000 rpm. The Matlab command fit([x, y], z, 'poly12') was used, which fits a polynomial surface of the first degree in X and second degree in Y. Inputting an X and Y value will output the Z value. For this calculation X represented engine speed (first order), Y represented MAP (second order), and Z represented torque. The linear fit for engine speed and quadratic fit for MAP were selected by comparing the surfaces to the actual torque curve. Engine speed and MAP input into the code would produce an estimation for the torque output. The Matlab code can be found in Appendix C. The MAP and engine speed from the dynamometer were first input into the surface fit to validate the surfaces. Figure 3.1 below shows the actual measured dyno torque compared to the estimated torque.

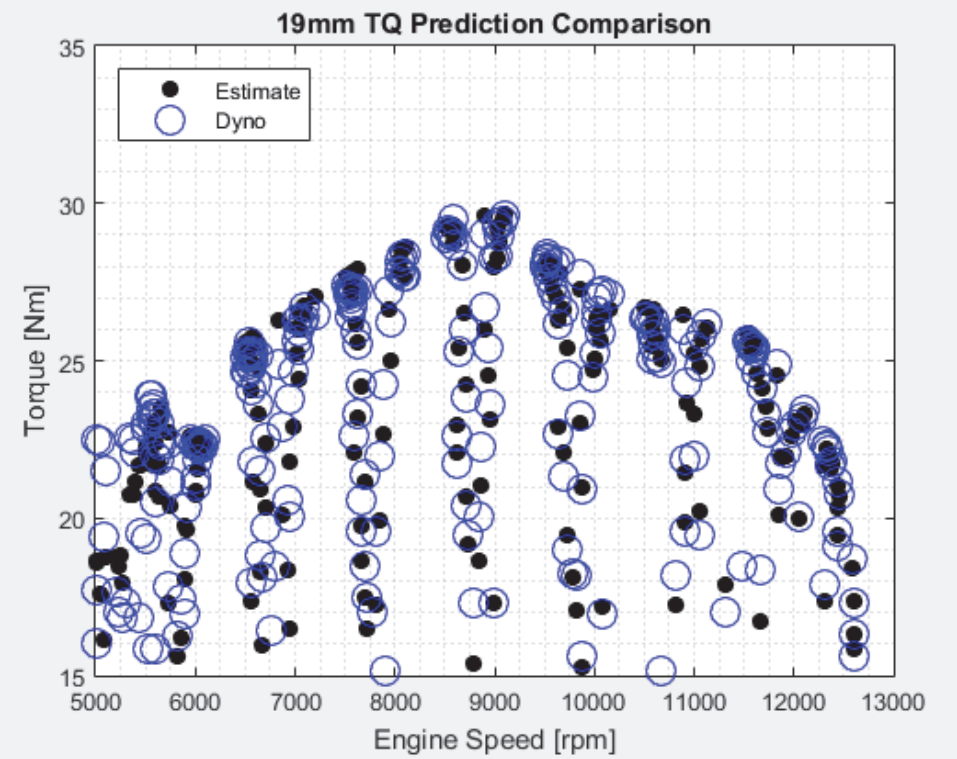

Figure 3.1: Comparison of estimated torque and measured torque for the same MAP and engine speed data.

The goodness of fit statistics for the different surface fits can be found in Appendix C. Once the surface fits were deemed acceptable, the on-track MAP and engine speed data was input into the code, and the estimated torque was generated. Figure 3.2 below shows the on-track torque compared to the actual torque available.

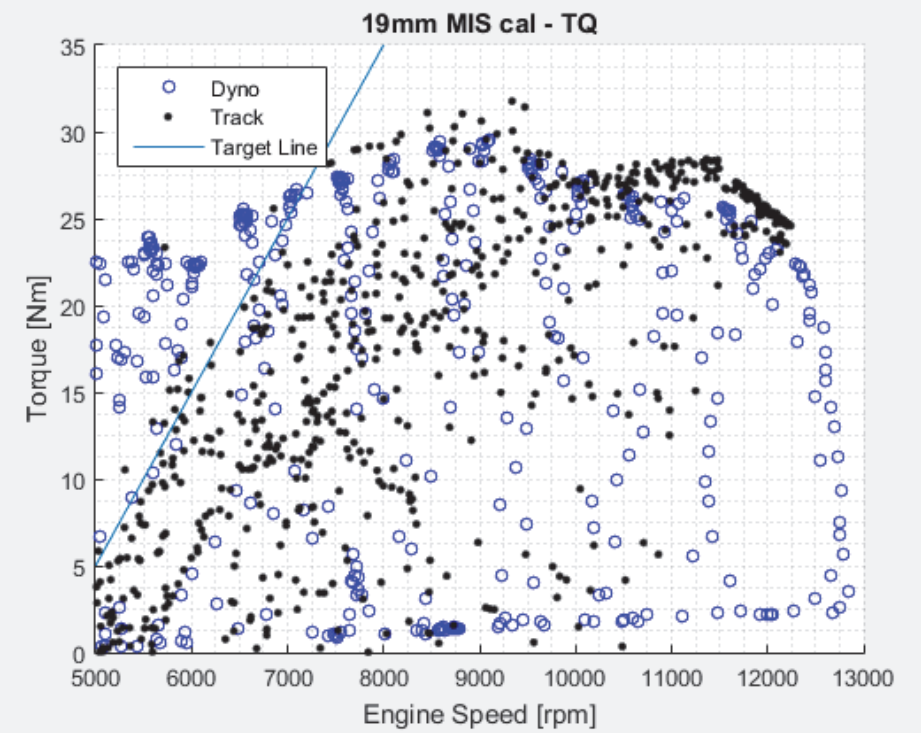

Figure 3.2: Engine torque used on-track compared to torque available.

As can be seen in Figure 3.2, the maximum amount of torque available is not fully used until above approximately 7,500 rpm. This is due to the driver trying to manage wheelspin with the throttle. Below 7,500 rpm the torque demanded by the driver increases in a linear fashion until the driver is using all of the available torque to maximum engine speed. This means there is much wasted torque that the driver was never able to use at low engine speeds.

The vehicle position data was downloaded from the AIM EVO4 DAQ into the software Race Studio 2, and was exported as a .gpx file, which Matlab was able to read. Since the GPS data was only recorded at 1 Hz, the position data was upsampled to 10 Hz using linear interpolation. This vehicle position data was then combined with the engine torque and speed data and used to generate color-coded track maps that indicate engine power used on track. Figure 3.3 shows the power used during a typical lap of the test track.

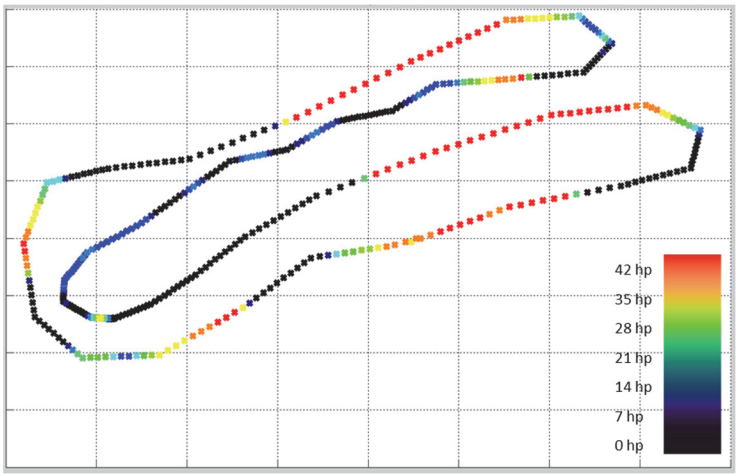

Figure 3.3: Engine power used for a typical lap of the CMX test track.

Figure 3.3 shows that the maximum engine power is utilized, but only on straights. To gain more insight into the power needed, a similar contour plot was developed depicting the 90th percentile of power, as Figure 3.4 shows.

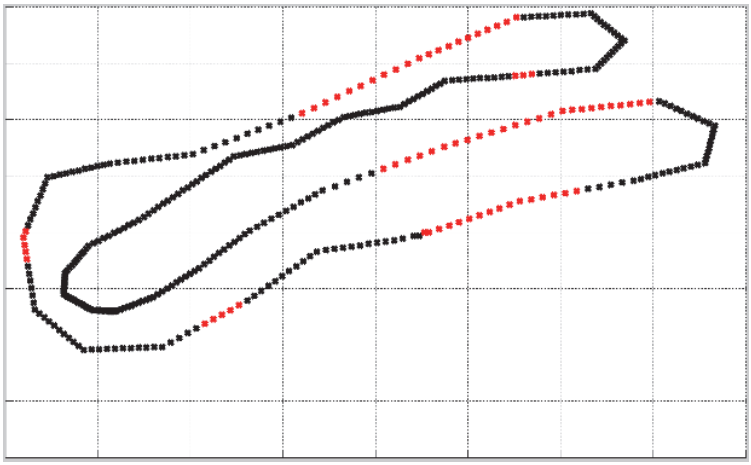

Figure 3.4: 90th percentile of engine power used for a typical lap of the CMX test track, with red being at or above 90% of maximum engine power, and black below.

From Figures 3.3 and 3.4 it can be determined that the full power of the engine is utilized if only for a partial amount of time per lap. This means an increase in maximum power will likely improve overall vehicle performance, if the torque target is also met. So for the development of the intake manifold the requirements determined were to follow the torque target line shown in Figure 3.2,

and because the air restrictor would limit maximum power at high engine speeds, generate as much peak power as possible without sacrificing the ideal torque curve.

3.2 Dynamometer Testing Results

The raw pressure data from ACAP was processed using Matlab by importing the .P01 files from ACAP into Matlab. Code was written to convert the individual .P01 files for crank angle, cylinder pressure, intake pressure, and exhaust pressure into a single Excel file with the data aligned. The Matlab code used to convert the files can be found in Appendix D. Once all the ACAP data was converted to Excel format, the cylinder pressure traces were plotted. Figure 3.5 shows the cylinder pressure traces for the engine being motored at approximately 300 rpm, and fired at 5,000, 8,000, and 11,000 rpm. The fired pressure traces at all speed points can be found in Appendix E.

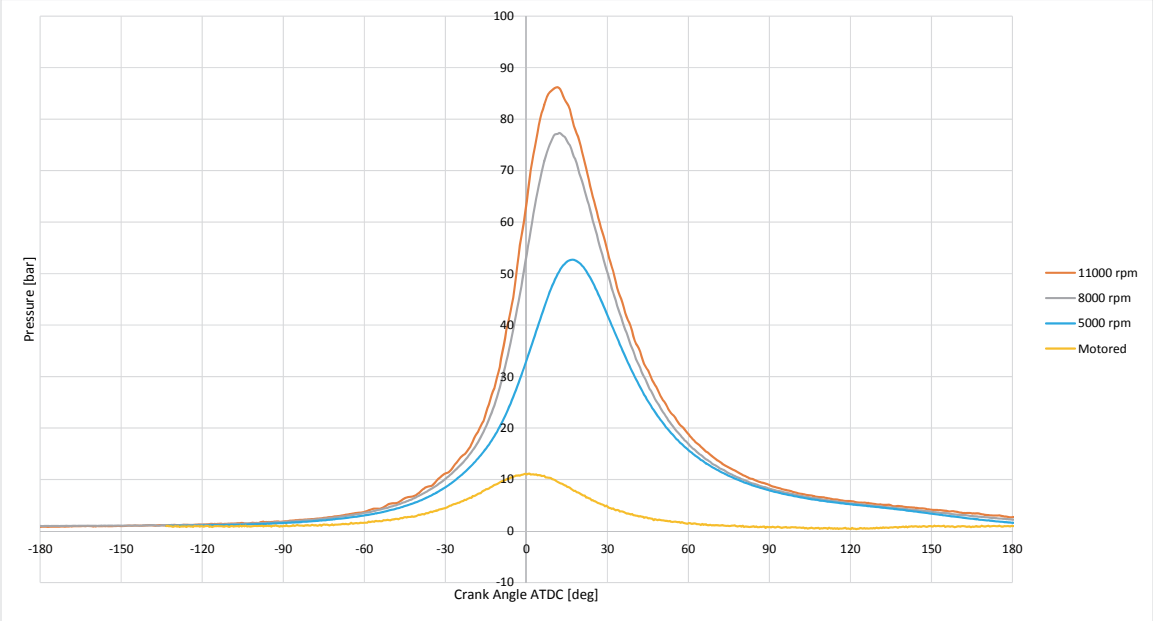

Figure 3.5: Yamaha Genesis 80 measured cylinder pressure versus crank angle motored and fired at 5,000, 8,000, and 11,000 rpm.

As can be seen in Figure 3.5, the measured cylinder pressures look as expected when plotted versus crank angle, meaning the encoder offset is correct. To further investigate the fidelity of the cylinder pressure data, a P-V diagram was produced based on the engine specifications, which can be found in Appendix B, and Equations 2.4 and 2.5 from Heywood. Figure 3.6 shows the P-V diagram for the ensemble average cylinder pressure at 8,000 rpm on a log-log scale.

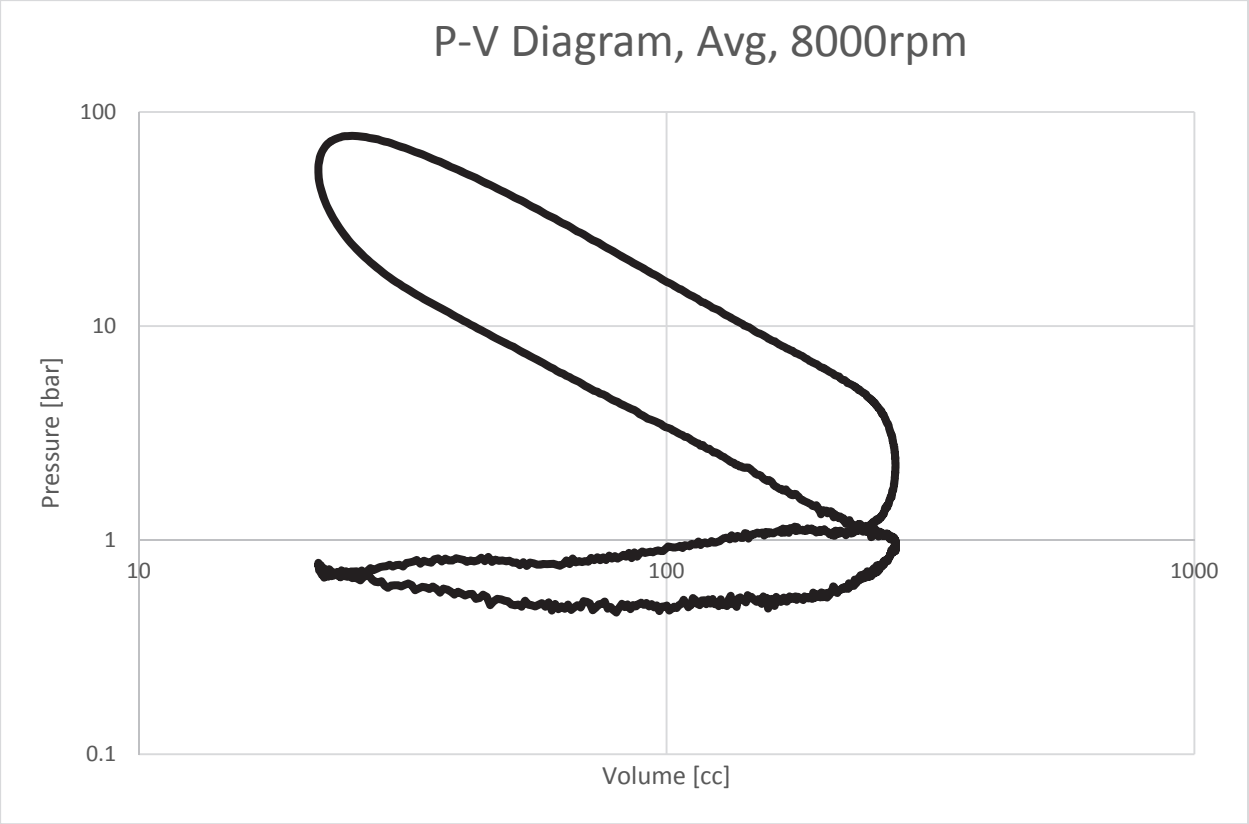

Figure 3.6: Ensemble averaged P-V diagram for 8,000 rpm.

Figure 3.6 shows the compression and expansion lines of the P-V diagram to be parallel, verifying the legitimacy of the cylinder pressure data. The combustion pressure data was then used to calibrate the GT-Power model.

3.3 GT-Power Model Calibration

The GT-Power model was calibrated based on AFR, fuel flow, VE, cylinder pressure, and torque output. The Wiebe function used to model combustion was tuned by adjusting CA50, D1090, and the Wiebe exponent. The CA50 and D1090 values calculated from the empirical cylinder pressure data were used as starting points.

3.3.1 Model Air and Fuel Flow Calibration

With the intake system and exhaust system accurately modeled in flow components, the AFR, fuel flow, and VE were closely matched to empirical data. Figure 3.7 below compares these parameters recorded on the dynamometer and predicted by GT-Power.

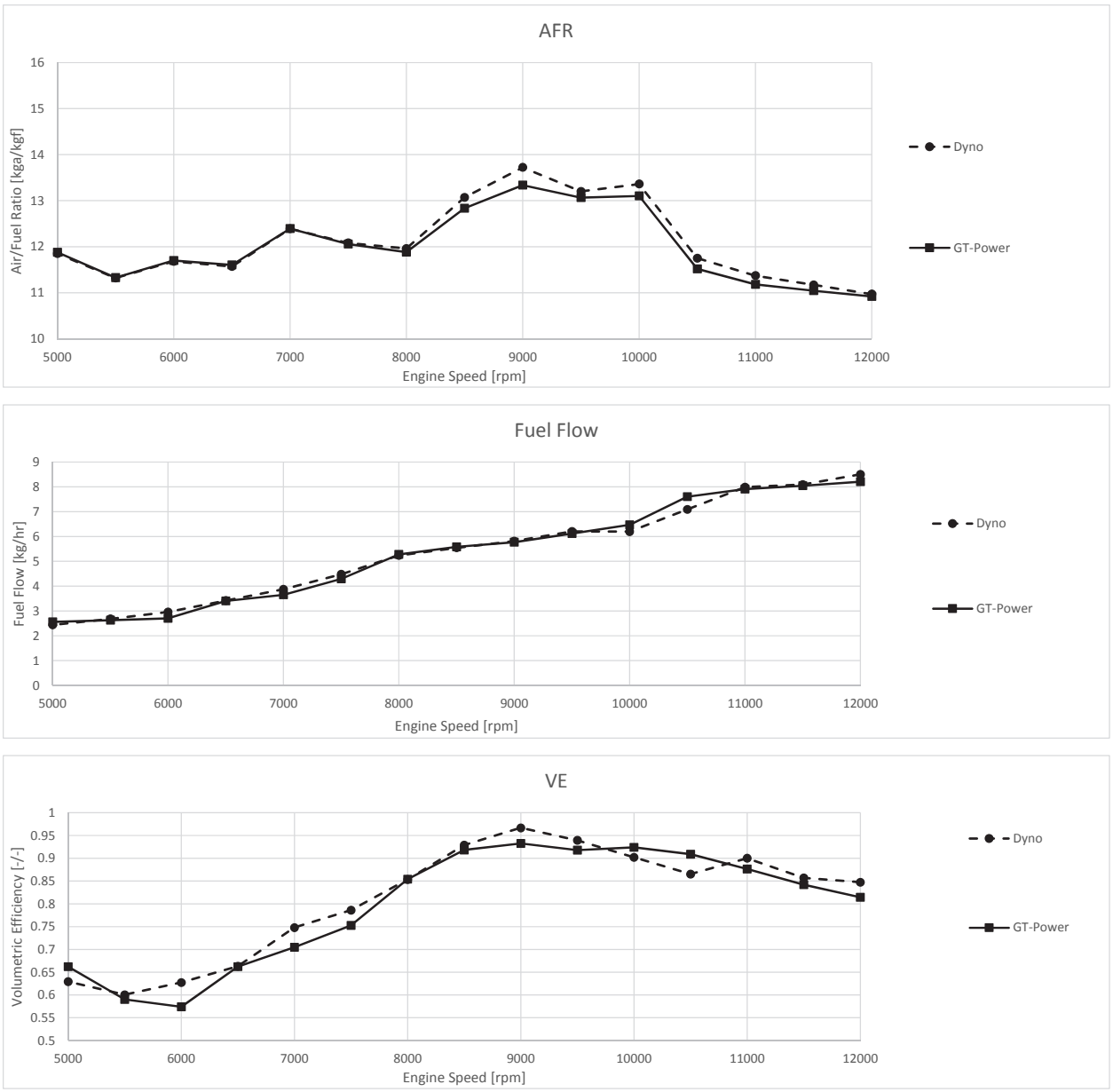

Figure 3.7: Empirical data versus GT-Power prediction for AFR, fuel flow, and volumetric efficiency.

3.3.2 Combustion Model Calibration

With the AFR, fuel flow, and VE closely aligned to the dynamometer data, the CA50 and D1090 values were then adjusted to match the predicted cylinder pressure to the empirical data. This was accomplished by sweeping CA50 and D1090 at each engine speed point and comparing the predicted cylinder pressure with the measured cylinder pressure. Table 3.1 lists the calculated

CA50 and D1090 values compared to the adjusted values used in GT-Power to match the cylinder pressure.

Table 3.1: Comparison of calculated and adjusted combustion parameters.

Engine Speed [rpm]	CA50 [crank angle degrees]		D1090 [crank angle degrees]	
	Calculated (dyno)	Adjusted (GT-Power)	Calculated (dyno)	Adjusted (GT-Power)
5,000	14.5	10.0	34.9	34.0
5,500	12.0	4.0	34.5	33.0
6,000	10.3	7.5	32.7	30.5
6,500	9.0	8.0	32.3	30.0
7,000	7.7	6.5	29.9	28.5
7,500	6.6	5.0	31.4	26.0
8,000	6.7	6.5	29.5	28.0
8,500	4.0	3.0	30.3	26.0
9,000	5.6	3.0	31.4	27.0
9,500	8.6	6.0	31.4	28.3
10,000	9.1	7.9	31.6	28.5
10,500	5.6	4.0	32.5	29.0
11,000	5.6	2.0	32.9	29.8
11,500	5.6	1.0	32.4	30.0

The CA50 and D1090 values used in GT-Power are inputs into the combustion model that represent the combustion process with a simplistic equation, and thus these values did not necessarily correlate with the actual values from the dynamometer. They are simply used to tune the predicted combustion process to match the actual cylinder pressure.

With the adjusted values of CA50 and D1090 shown in Table 3.1, the predicted cylinder pressure was closely matched to the measured data. Figures 3.8-3.10 show the measured and predicted cylinder pressure curves versus crank angle for 11,000, 8,000, and 5,000 rpm. The pressure comparisons for the other engine speed points can be found in Appendix E.

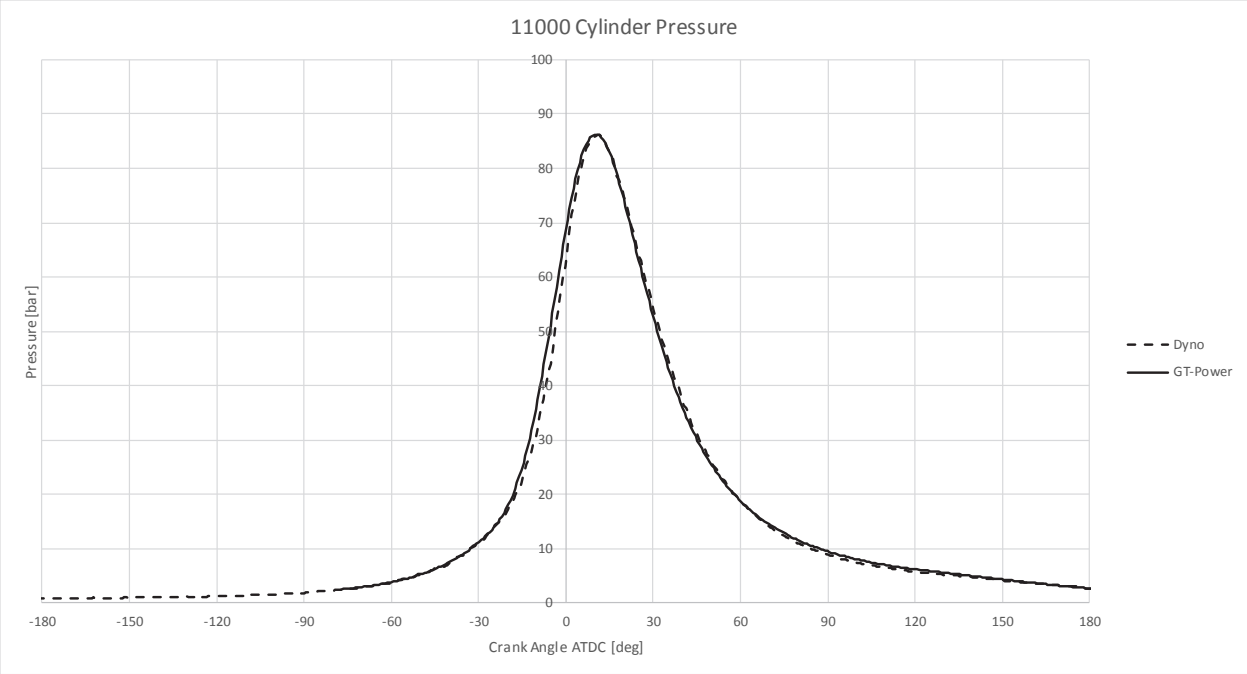

Figure 3.8: Measured versus predicted cylinder pressure at 11,000 rpm.

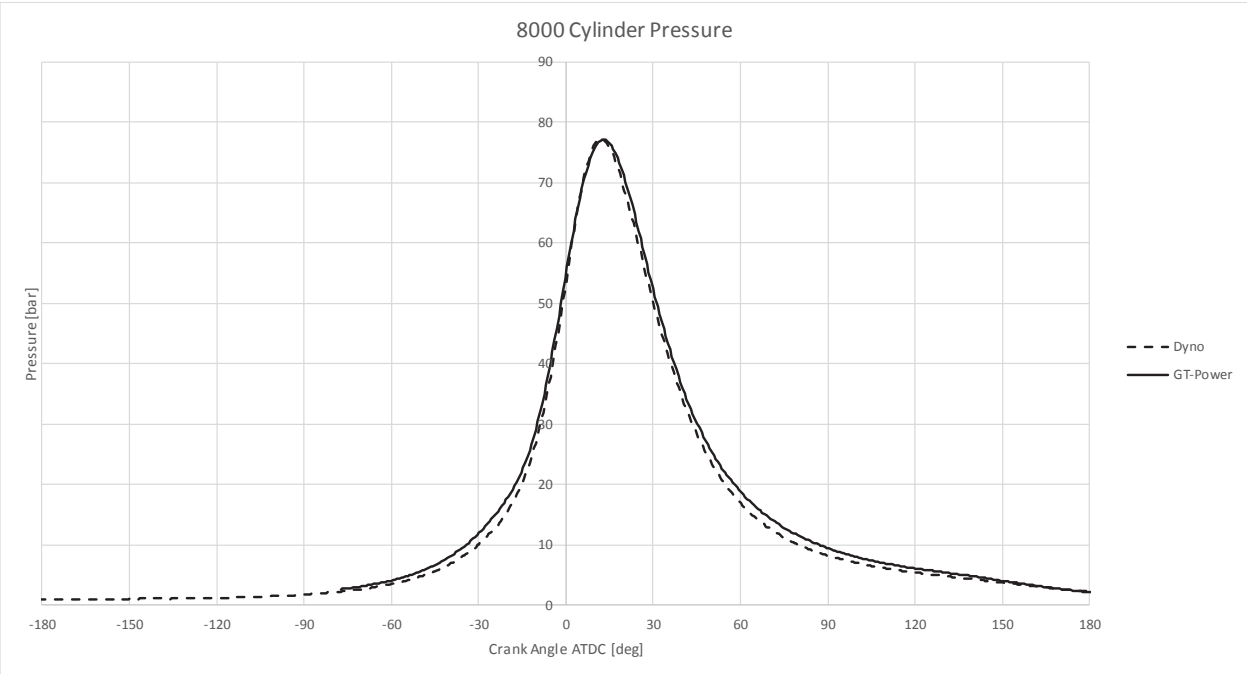

Figure 3.9: Measured versus predicted cylinder pressure at 8,000 rpm.

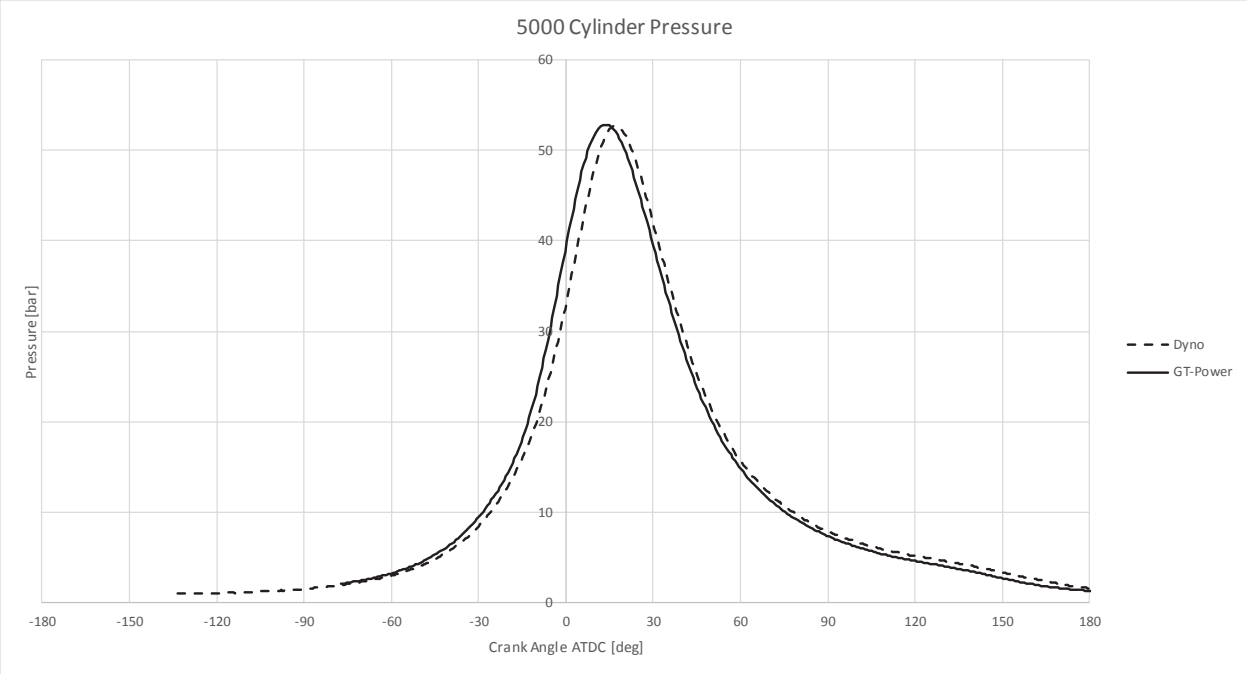

Figure 3.10: Measured versus predicted cylinder pressure at 5,000 rpm.

As Figures 3.8-3.10 show, there were slight discrepancies in the pressures during the compression stroke, however the GT-Power predictions did not include any blow-by, resulting in a slight inflation of the slope of the pressure curve because it models perfect sealing of the rings. To accurately model the blow-by a blow-by meter would be needed, which was unavailable at the time. Despite this, the predictions were able to match the peak cylinder pressures closely.

3.3.3 Torque Calibration

With the AFR, fuel flow, VE, and cylinder pressures calibrated, the final calibration was the torque, which was fine-tuned using the friction modeled in GT-Power. The friction was modeled with the Chen-Flynn friction model, which calculates FMEP based on a constant, maximum cylinder pressure, and mean piston speed. GT-Power recommends factors to start with, and only slight adjustment was necessary to match the predicted torque to the measured torque. Table 3.2 shows the initial and final values used in the Chen-Flynn model.

Table 3.2: Friction factors used in GT-Power to fine tune torque output.

Factor	Initial Value	Final Value
FMEP Constant [bar]	0.5	0.5
Peak Cylinder Pressure	0.005	0.005
Mean Piston Speed [bar/(m/s)]	0.09	0.14
Mean Piston Speed Squared [bar/(m/s^2)]	0.0009	0.0008

With these friction factors and the AFR, fuel flow, and cylinder pressure closely matched to the empirical data, the torque also matched closely to the measured values. Figure 3.11 shows the comparison of predicted and measured torque.

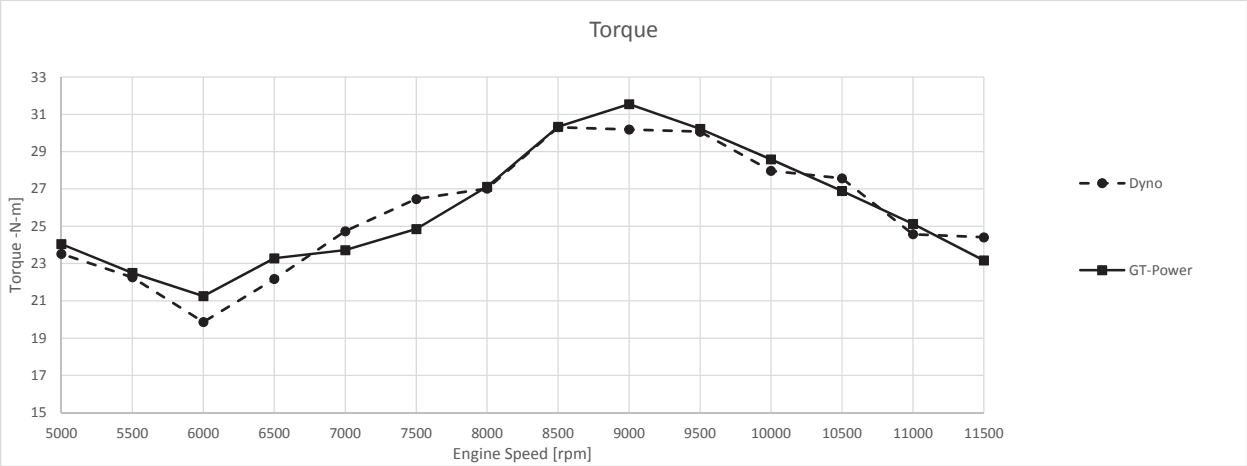

Figure 3.11: Comparison of predicted and measured torque with the GT-Power model calibrated.

With the predicted torque following the actual torque curve, the combustion model was then used to refine the intake geometry.

3.4 Intake Geometry Refinement Results

From the intake manifold geometry DOE the ideal dimensions were found to be runners 140 mm long with 50 mm inlet diameters. To package the runners in the vehicle without negatively impacting performance a 70 mm radius of curvature was used with 90° bends plus 30 mm of

straight runner. Figure 3.12 shows the predicted torque curve of the new (F260) intake compared to the predicted F194 torque curve.

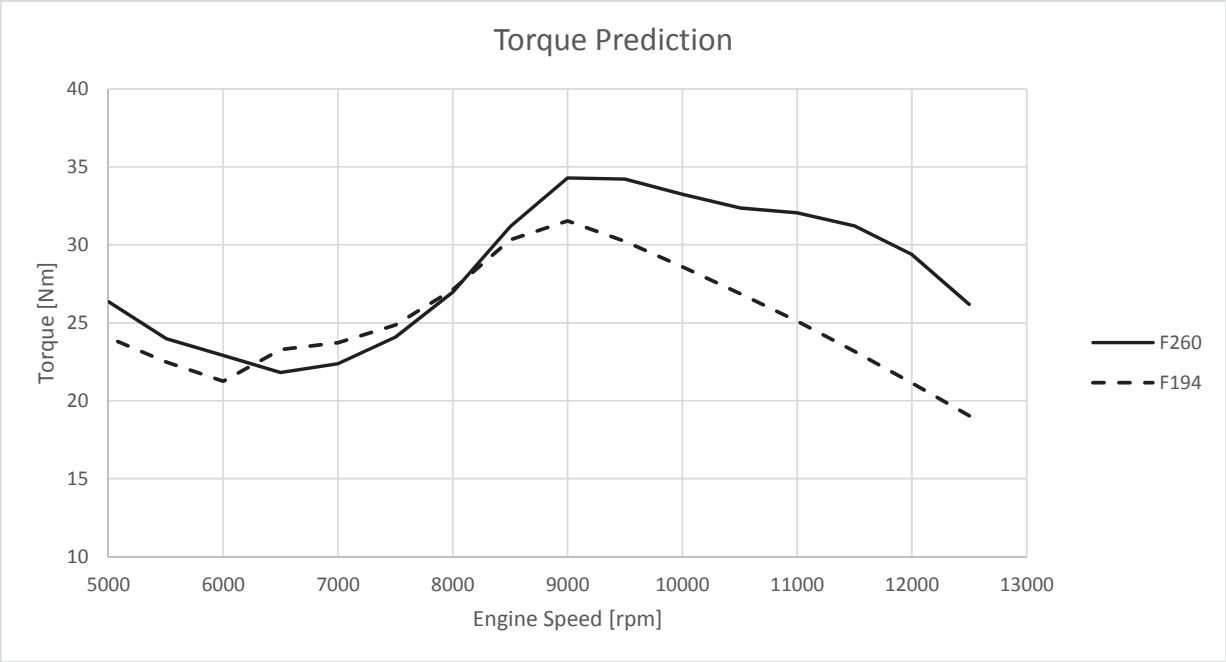

Figure 3.12: Torque comparison between old F194 and new F260 geometry.

As the figure shows the new geometry follows the target line longer than the previous design, producing less torque from about 6,250 rpm to 8,000 rpm and 9 to 9 N-m more torque past 9,000 rpm. The new geometry should allow the vehicle to continue accelerating for longer while the reduced torque at lower engine speeds should improve drivability. Based on the results of the GT-Power study a 3-D CAD model was then developed of the refined intake manifold.

3.5 CAD Model Development and 3-D Printing

Using Siemens NX 10, a 3-D model of the intake manifold was developed featuring the geometry found with GT-Power. Figure 3.13 shows the final 3-D model.

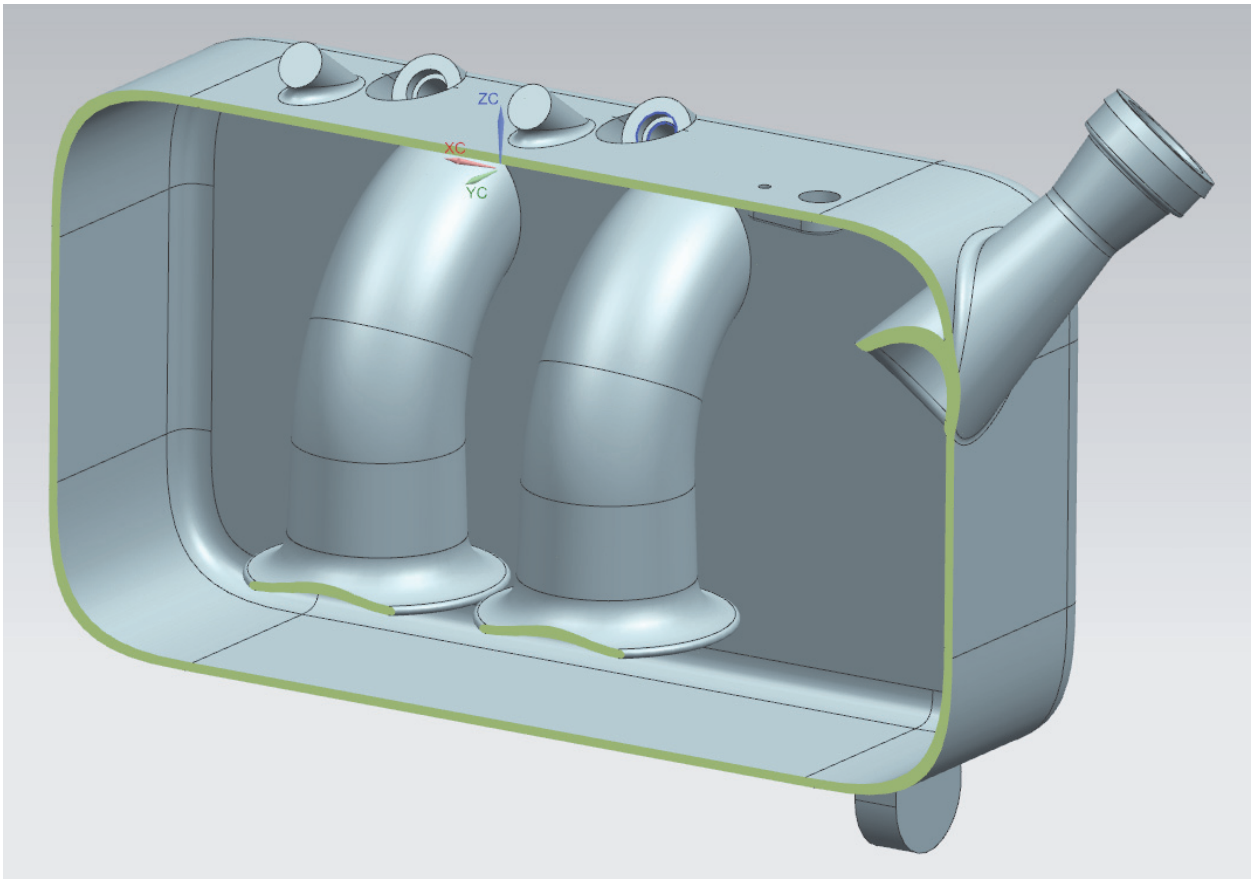

Figure 3.13: Final CAD model of the F260 intake manifold, made in Siemens NX 10.

The F260 intake manifold features internal runners for compact packaging, bosses for mounting the fuel rail, bungs for the fuel injectors, a mounting tab, 20 mm intake air restrictor, and allocations for a MAP sensor. Table 3.3 highlights the dimensional differences between the new intake F260 intake design and the previous MTU FSAE intake manifolds.

Table 3.3: Intake manifold geometry of MTU FSAE vehicles.

Dimension	F194 (2015)	F315 (2016)	F260 (2017)
Runner Length [mm]	220	300	140
Runner Inlet Diameter [mm]	49	54	50
Runner Radius of Curvature [mm]	55	50	70
Plenum Volume [L]	3.0	3.2	5.3

Once the CAD model was finalized, a high-resolution .stl file was exported, which is required for 3-D printing. McLaren Engineering in Livonia, MI printed the intake manifold using a Stratasys Fortus 400mc fused deposition modeling printer. The plastic is Polycarbonate-ABS and is resistant

to gasoline and the temperatures an intake manifold might experience in a FSAE vehicle. Figure 3.14 shows the final printed manifold.

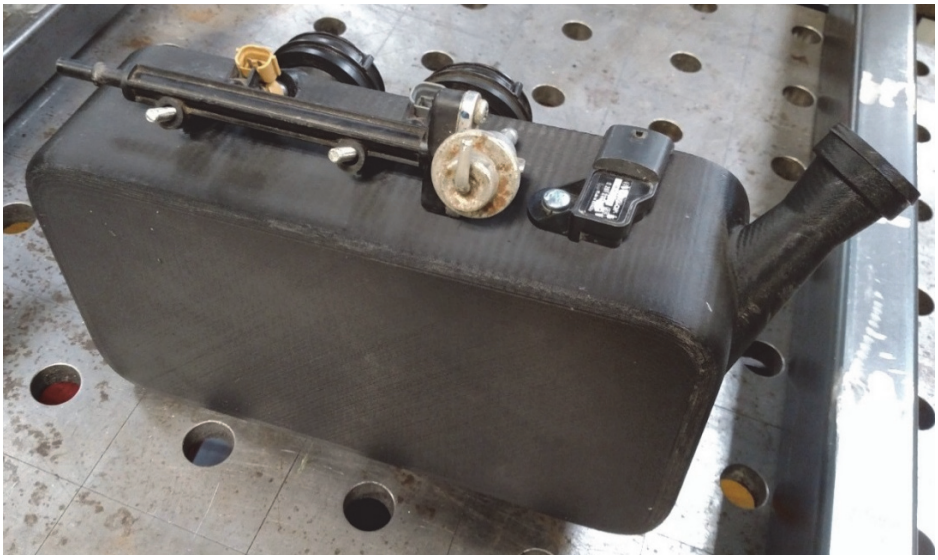

Figure 3.14: 3-D printed F260 intake manifold, with fuel injectors, fuel rail, and MAP sensor installed.

The intake manifold was test fit in the vehicle to verify fitment, as Figure 3.15 shows.

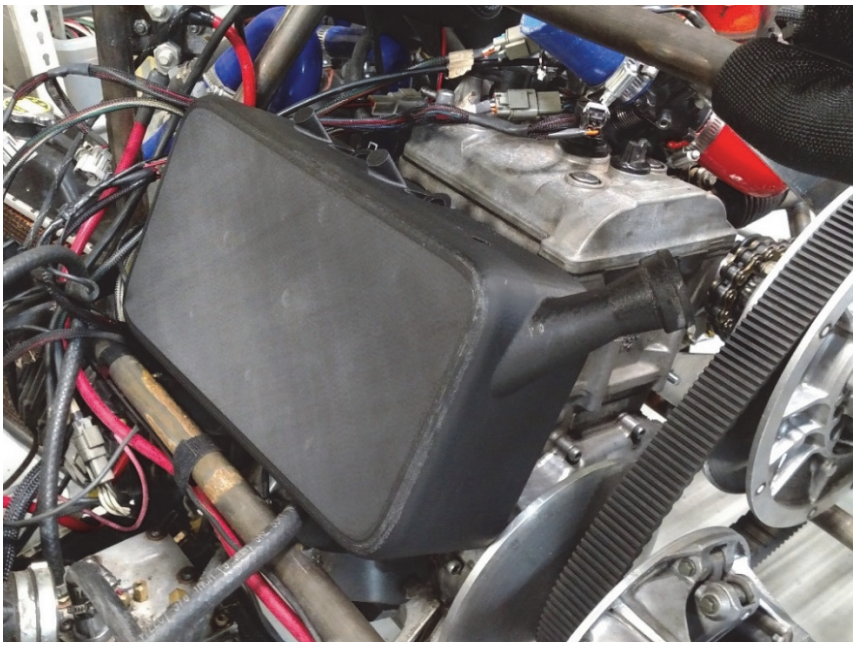

Figure 3.15: F260 intake manifold in the race vehicle.

3.6 Performance Comparison

3.6.1 Dynamometer Performance Comparison

To compare the actual torque produced by the engine with the new intake manifold, the fuel delivery and ignition timing were calibrated on the dynamometer. With a rough base calibration completed, a sweep of the engine speed at wide open throttle was then performed to record the torque curve. Figure 3.16 shows the torque curve with the F260 intake manifold, as recorded with the water brake dynamometer compared to the predicted torque output from GT-Power.

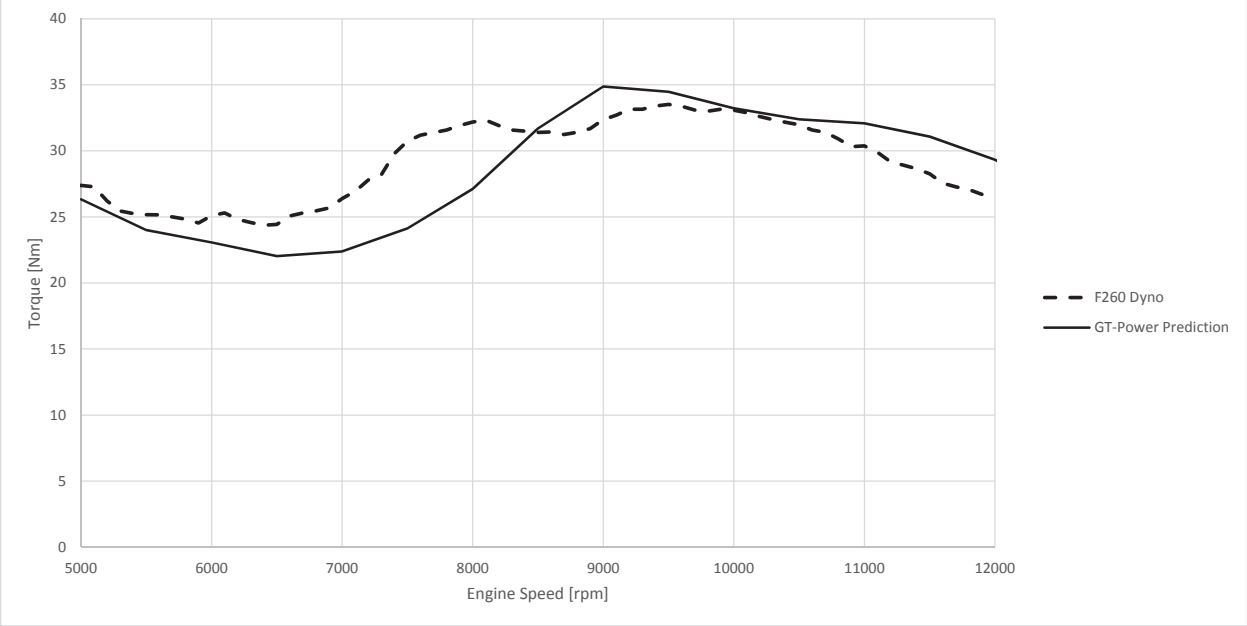

Figure 3.16: Comparison of torque predicted by GT-Power and the torque measured on the dynamometer with the F260 intake manifold.

While the torque curve produced by the engine with the F260 intake manifold followed a similar shape as predicted by GT-Power, it differed by as much as 27.4% at 7,500 rpm.

After the engine speed sweep the throttle was closely closed and the large pressure difference between the manifold and atmosphere as the throttle closed caused the bottom of the plenum to crack, allowing unmetered air into the engine and resulting in a loss of control of the engine speed. The time required to repair the intake manifold for track testing meant the calibration was not able to be further refined. Figure 3.17 shows the cracked intake manifold during repair.

Figure 3.17: Cracked F260 intake manifold being repaired by epoxy.

Note the epoxy used to repair cracked manifold in Figure 3.17. Once the epoxy sealing the cracks dried, a piece of sheet metal was bent to fit on the bottom and front/back on the plenum, and epoxied onto the plastic to add stiffness.

3.6.2 On-Track Performance Comparison

With the fuel and spark safely calibrated and the cracked F260 intake manifold repaired, an on-track comparison was attempted. The test track shown in Figure 2.2 was again setup at CMX to be used for comparing the F315 intake manifold with the F260 intake manifold on the same vehicle. Due to the fragility of the intake manifold, it was decided to alter the test plan.

The driver practiced on the track with the F315 intake manifold until lap times became consistent, starting at 40.71 seconds per lap and stabilizing at 32.42 seconds per lap after 13 laps. The repaired F260 intake manifold was then installed on the vehicle and the driver attempted a timed lap, however the manifold cracked under vacuum again about three quarters of the way through the lap and the driver began to lose control of the engine. The lap was completed in 39.54 seconds, which shows the new intake is on pace with the old intake, but because this was the only lap completed the lap time differences with the new intake cannot be determined at this time.

Chapter 4

Conclusions and Recommendations

4.1 Conclusions

From this project it can be concluded that recording engine speed and MAP is an accurate way to determine torque usage on-track, and can be very useful for development of the engine from a vehicle performance stand point.

To develop the intake manifold design, 1-D engine simulations such as GT-Power can be useful, and the Wiebe function can be used to accurately calibrate a model to match the simulated and measured cylinder pressure. However, the use of a full engine model based around the Wiebe function has limitations in accurately predicting torque when limited information regarding the engine geometry, thermal properties, and airflow characteristics is available.

4.2 Recommendations

To gain more insight into the 1-D engine model, the intake, cylinder, and exhaust pressures should be recorded using the high-speed ACAP data acquisition system and compared to predicted values from GT-Power. This could point to the cause of the discrepancy in torque from 6,000 to 10,000 rpm between the model and actual engine.

Due the intake manifold cracking under vacuum, a structural analysis of the intake manifold needs to be done. A revised design, likely featuring more curvature and increased wall thickness will need to be developed for use on the vehicle. Finite Element Analysis can be done, and it is recommended to perform material property tests using samples from the 3-D printer system, such as an old FSAE intake manifolds no longer in use. With a structurally sound intake manifold the on-track comparison should be completed, again comparing the different intake manifolds with

the consistent drivers, track, and conditions. A refined fuel and spark calibration will also improve the quality of the comparison.

To improve the engine testing capabilities of the MTU FSAE team, dynamometer cell improvements can be made. These include fuel flow measurement, airflow measurement, and a combustion air system to regulate air temperature and humidity.

References

[1] J. B. Heywood, Internal Combustion Engine Fundamentals, McGraw-Hill, 1988, p. 312.

[2] J. B. Heywood, Internal Combustion Engine Fundamentals, McGraw-Hill, 1988, p. 218.

[3] S. International, "Formula SAE Michigan," 2015. [Online]. Available: http://students.sae.org/cds/formulaseries/fsae/.

[4] Heywood, Internal Combustion Engine Fundamentals, McGraw-Hill, 1988, p. 768.

Appendix A

Engine Instrumentation Information

A.1 Encoder, Mount and Adaptor Shaft Drawings

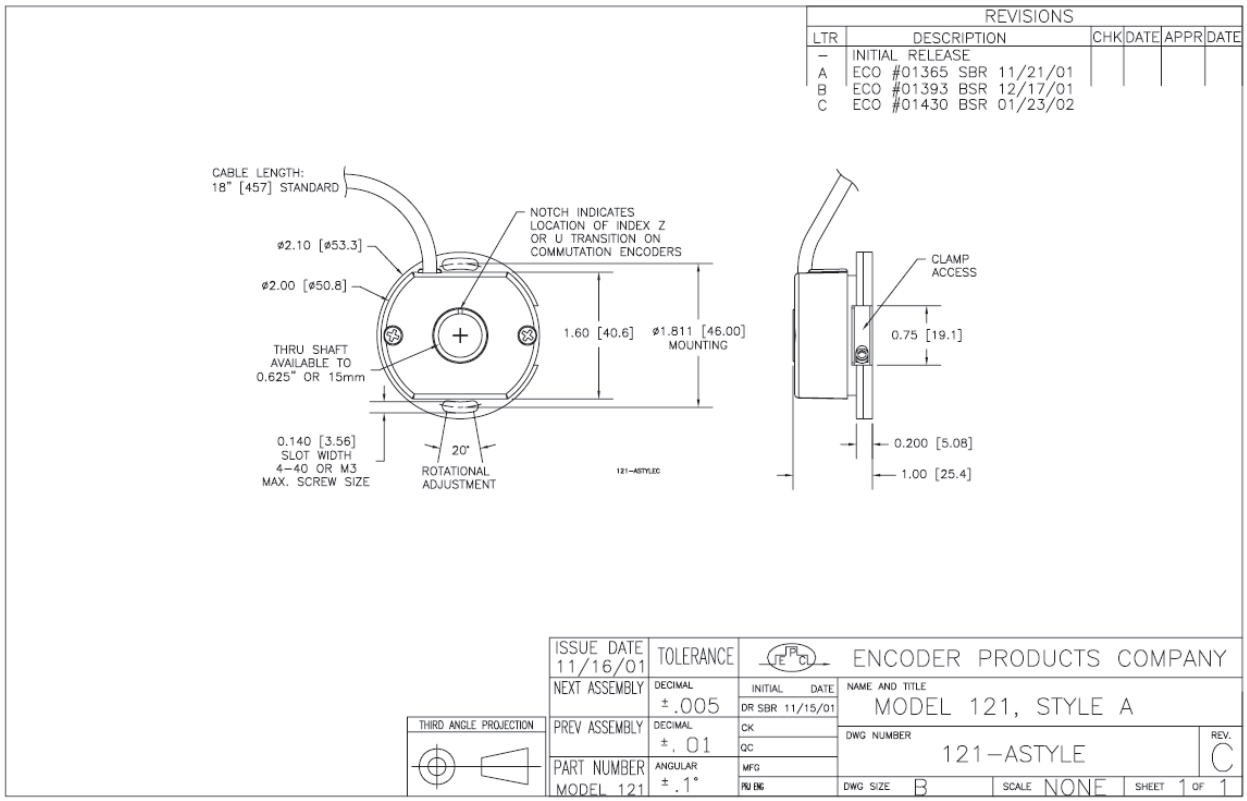

Figure A.1: Encoder Products Model 121 drawing.

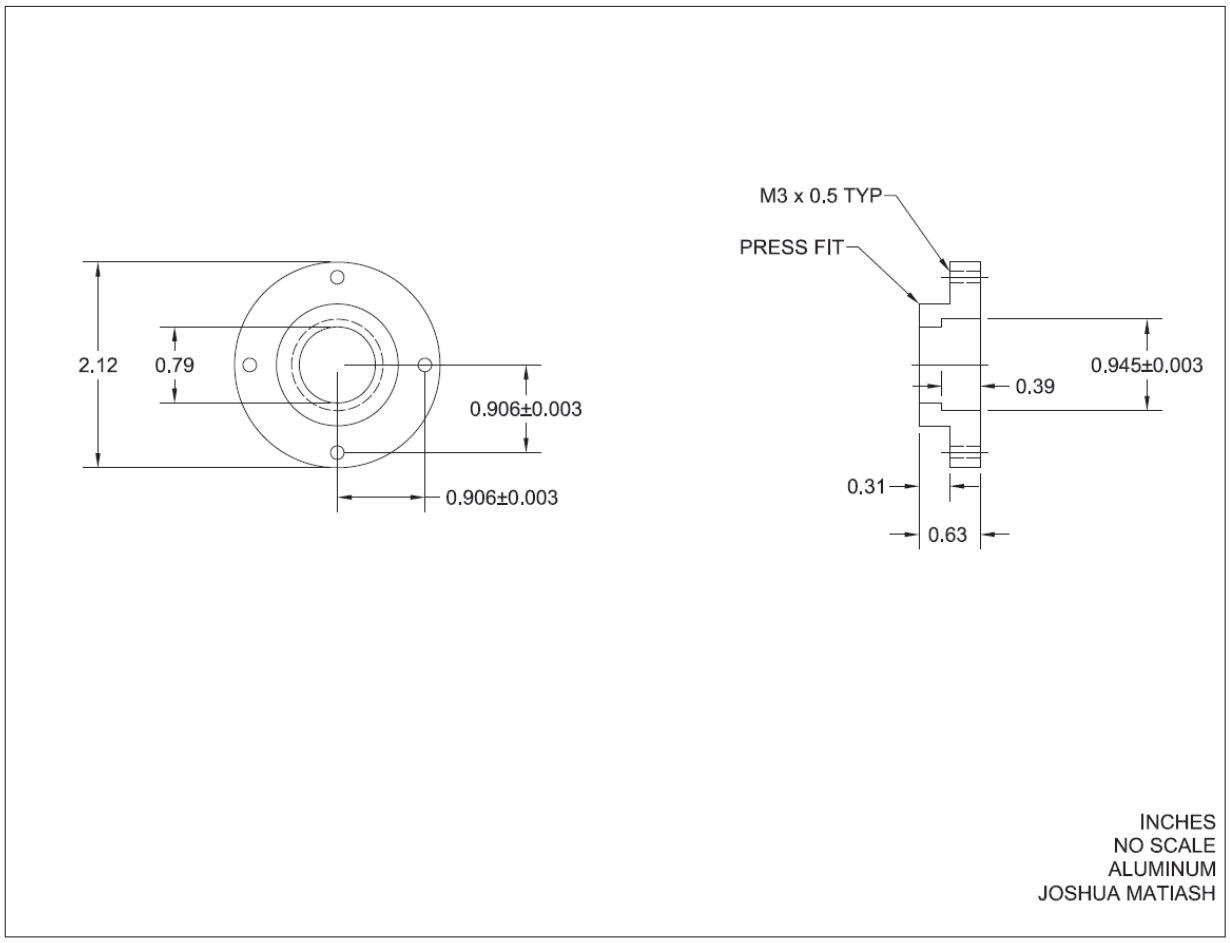

Figure A.2: EPC 121 crankshaft encoder mount for a Yamaha Genesis 80.

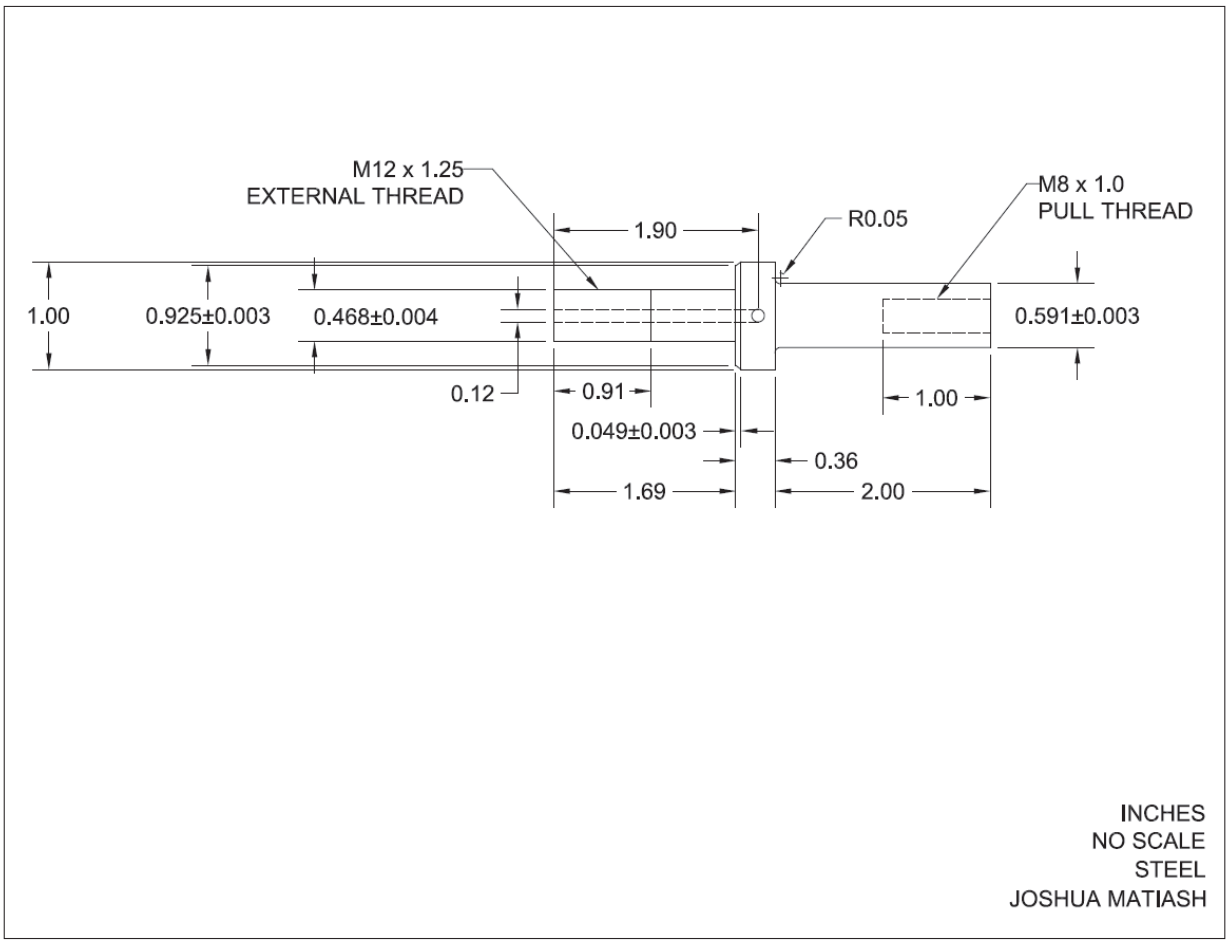

Figure A.3: EPC 121 crankshaft encoder shaft adaptor for a Yamaha Genesis 80.

A.2 Kulite Pressure Transducer Drawings

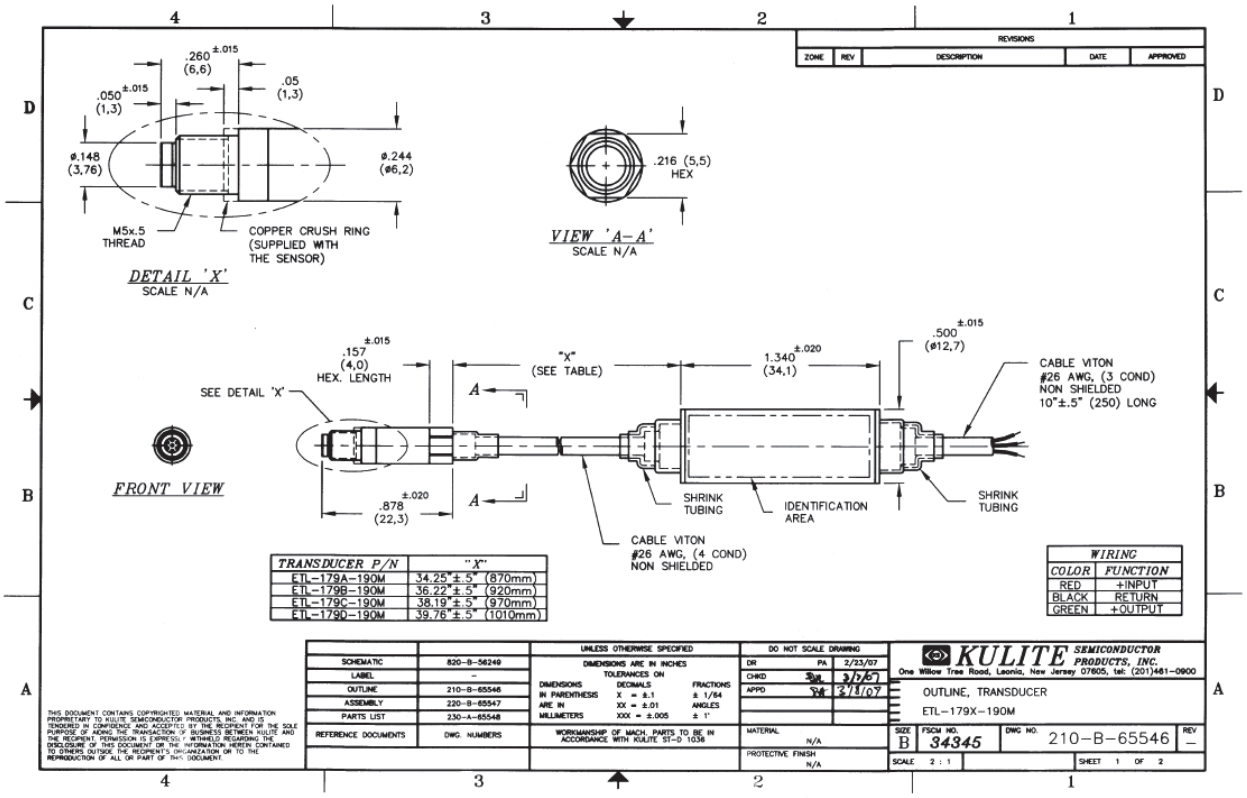

Figure A.4: Kulite ETL179x-190M pressure transducer drawing.

kulite

WATER/AIR COOLED 5VDC OUTPUT TRANSDUCER

EWCTV-312 (M)

- High Bandwidth With Integrated Amplifier
- Patented Leadless Technology **VIS®**
- Superior Thermal Protection
- Both Dynamic and Static Output Capabilities
- Extreme Temperature Capabilities Such As Required In Exhaust Systems

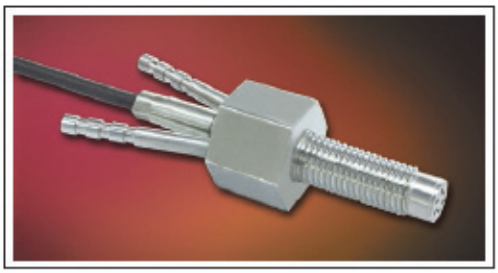

Kulite Introduces a new compact Water Cooled Pressure Transducer for both dynamic and static pressure measurements in extreme temperature environments such as automotive and turbine exhaust systems. The EWCTV-312 combines Kulite's patented Leadless Silicon Technology and a Miniature Water Cooled Jacket to provide pressure measurement capabilities previously unavailable.

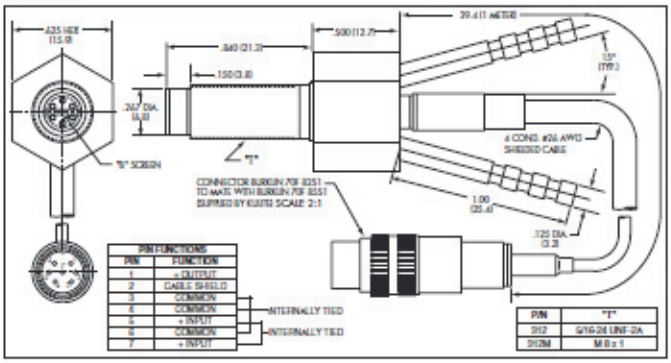

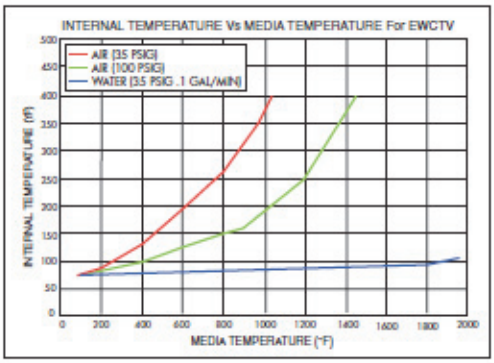

INPUT	Pressure Range	1.7 25	3.5 50	7 100	14 200	21 300	35 500	70 1000	140 BAR 2000 PSI
	Operational Mode	Absolute, Sealed Gage							
	Over Pressure	2 Times Rated Pressure							
	Burst Pressure	3 Times Rated Pressure							
	Pressure Media	Compatible With Exhaust Gases and Fluids and Most Liquids and Gases Compatible With SiO^2 And 15-5 PH Stainless Steel (Please Consult Factory)							
	Maximum Electrical Current	25mA							
	Rated Electrical Excitation	12 ± 4 VDC		28 ± 4 VDC			28 ± 4 VDC		
OUTPUT	Full Scale Reading	5 V ± 150mV		5 V ± 150mV			10 V ± 300mV		
	Output Impedance	200 Ohms (Nom.)							
	Frequency Response	Flat to 5000 Hz (±2dB) Typical							
	Residual Unbalance	0.5V ±100mV							
	Combined Non-Linearity, Hysteresis and Repeatability	± 0.1% FSO BFSL (Typ.) ± 0.5% FSO (Max.)							
	Resolution	Infinitesimal							
	Insulation Resistance	100 Megohm Min. @ 50 VDC							
ENVIRONMENTAL	Operating Temperature Range	75°F to +2000°F (24°C to +1093°C) (Front End) -4°F to +185°F (-20°C to +85°C) (Connector and Amplifier)							
	Water Flow Rate	.15 Gal/Min (Typ.)							
	Linear Vibration	10-2,000 Hz Sine, 100g. (Max.)							
	Mechanical Shock	20g half Sine Wave 11 msec. Duration							
PHYSICAL	Electrical Connection	Burklin 70F 8251 Connector (Mating Connector Supplied)							
	Weight	50 Grams (Approx.) Excluding Cable and Connector							
	Pressure Sensing Principle	Fully Active Four Arm Wheatstone Bridge Dielectrically Isolated Silicon on Silicon Patented Leadless Technology							
	Mounting Torque	50 Inch-Pounds (Max.) 6Nm							

Note: Custom pressure ranges, accuracies and mechanical configurations available. Dimensions are in inches. Dimensions in parenthesis are in millimeters. All dimensions nominal. (H) Continuous development and refinement of our products may result in specification changes without notice.
Kulite miniature pressure transducers are intended for use in test and research and development programs and are not necessarily designed to be used in production applications. For products designed to be used in production programs, please consult the factory.

KULITE SEMICONDUCTOR PRODUCTS, INC. • One Willow Tree Road • Leonia, New Jersey 07605 • Tel: 201 461-0900 • Fax: 201 461-0990 • http://www.kulite.com

Figure A.5: Kulite EWCTV-312M pressure transducer spec sheet.

Appendix B

Yamaha Genesis 80 Information

Table B.1: Yamaha Genesis 80 specifications.

Engine Configuration	Parallel Twin, Odd Fire
Displacement	499 cc
Bore	77.0 mm
Stroke	53.6 mm
Connecting Rod Length	100.0 mm
Compression Ratio	12.4:1
Valvetrain	DOHC, 5 Valves Per Cylinder
Intake Camshaft Centerline	466.5 cad
Exhaust Camshaft Centerline	258 cad

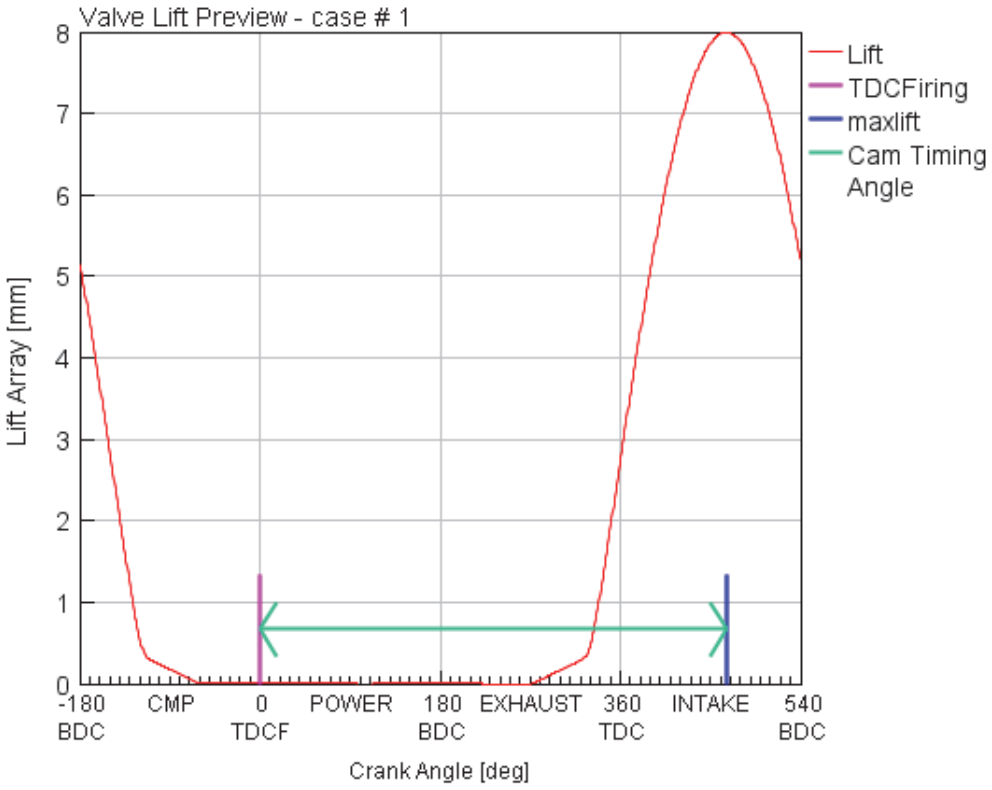

Figure B.1: Yamaha Genesis 80 intake camshaft profile.

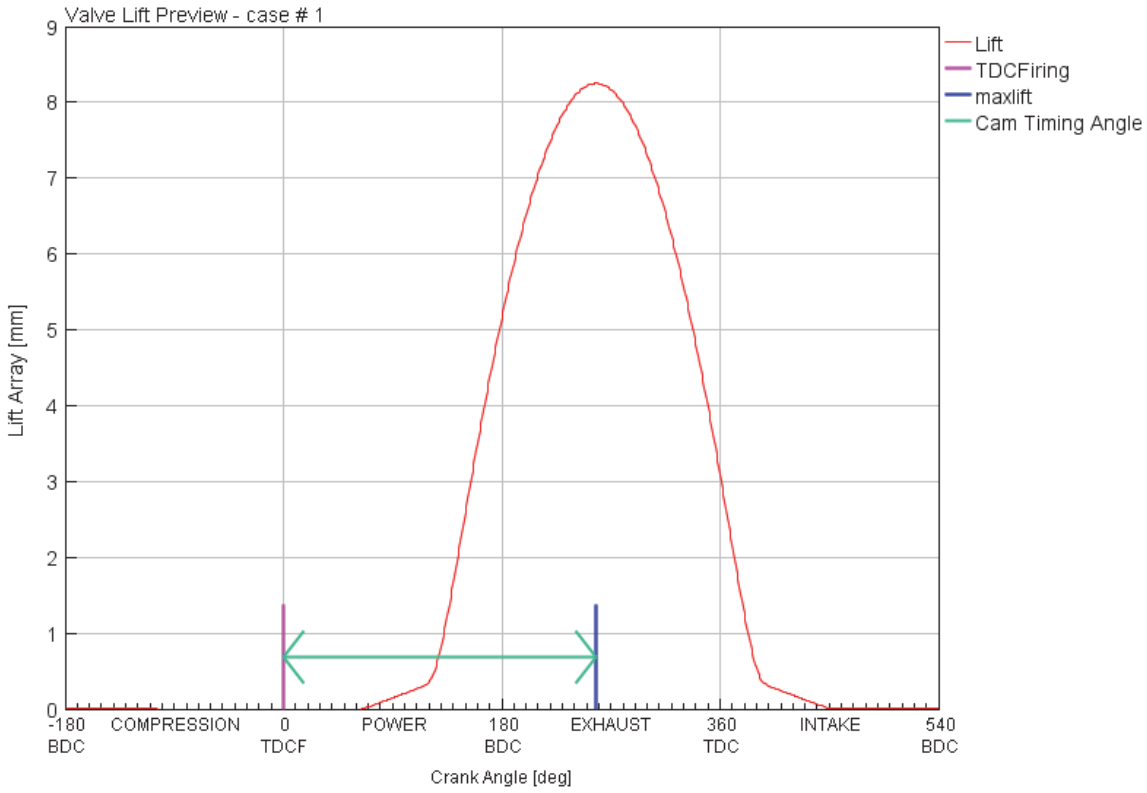

Figure B.2: Yamaha Genesis 80 exhaust camshaft profile.

Appendix C

Additional Torque Usage Information

Sample Matlab code for torque usage surface fit.

```
%Load dyno data
x = ENGINESPEED(2:end);  %engine speed on dyno
y = MAPkpa(2:end);       %manifold absolute pressure on dyno
z = CORPWRHP(2:end);     %engine power on dyno

sf = fit( [x, y], z, 'poly32' ); %this fits a surface to the dyno data
                                 %to be used to estimate on-track power

%Load on track engine speed and MAP data

u = PErpm;  %engine speed on track
v = PEmap;  %manifold absolute pressure on track

TrackPWR = sf(u,v); %engine power on track
```

Table C.1: Goodness of fit statistics for the torque usage surface fits.

Speed Range [rpm]	<4,600	4,600-5,300	5,301-5,700	5,701-6,500	6,501-8,500	8,501-9,500	9,501-10,000	10,001-11,500	11,501-13,000
SSE	169.99	391.93	136.09	46.91	371.66	62.18	8.3707	160.92	17.33
R^2	0.9198	0.8531	0.9324	0.9833	0.9701	0.9945	0.9961	0.9757	0.9964
DFE	48	38	28	28	113	66	23	58	54
Adjusted R^2	0.9131	0.8377	0.9227	0.9809	0.9690	0.9942	0.9954	0.9740	0.9961
RMSE	1.8819	3.2115	2.2046	1.2943	1.8136	0.9707	0.6033	1.6657	0.5666

Appendix D

Matlab Code to Convert ACAP Files to Excel Files

```
%Joshua Matiash
%MTU FSAE
%ACAP to .xlsx file converter

clear
close all
clc

%Specify folder the data is located in
TEST = ['M:\fsae\SubTeams\President\Research\Dyno Testing
MEEM\9_20\DATA54\']; %specify folder  %CHANGE ME

%load the .P01 files output by ACAP
load('-mat', [TEST sprintf('TQ01.P01')]); %load cyl pres

load('-mat', [TEST sprintf('TQC02_.P01')]); %load int pres

load('-mat', [TEST sprintf('TQC04_.P01')]); %load exh pres

load('-mat', [TEST sprintf('TQRWENCD.P01')]); %load CA

plot(TQRWENCD001(216000:217440),TQ01001(216000:217440))

max=max(TQ01001)
%%
%outputs data into single excel file
filename = 'Motored25_F194.xlsx';  %name excel file
%CHANGE ME
A=TQRWENCD001; %crank angle
B=TQ01001; %cylinder pressure
C=TQC02_001; %intake pressure
D=TQC04_001; %exhaust pressure
```

```
xlswrite(filename,A,['a2:a' num2str(length(A))]);

xlswrite(filename,B,['b2:b' num2str(length(B))]);

xlswrite(filename,C,['c2:c' num2str(length(C))]);

xlswrite(filename,D,['d2:d' num2str(length(D))]);
```

Appendix E

Cylinder Pressure Traces and Comparison

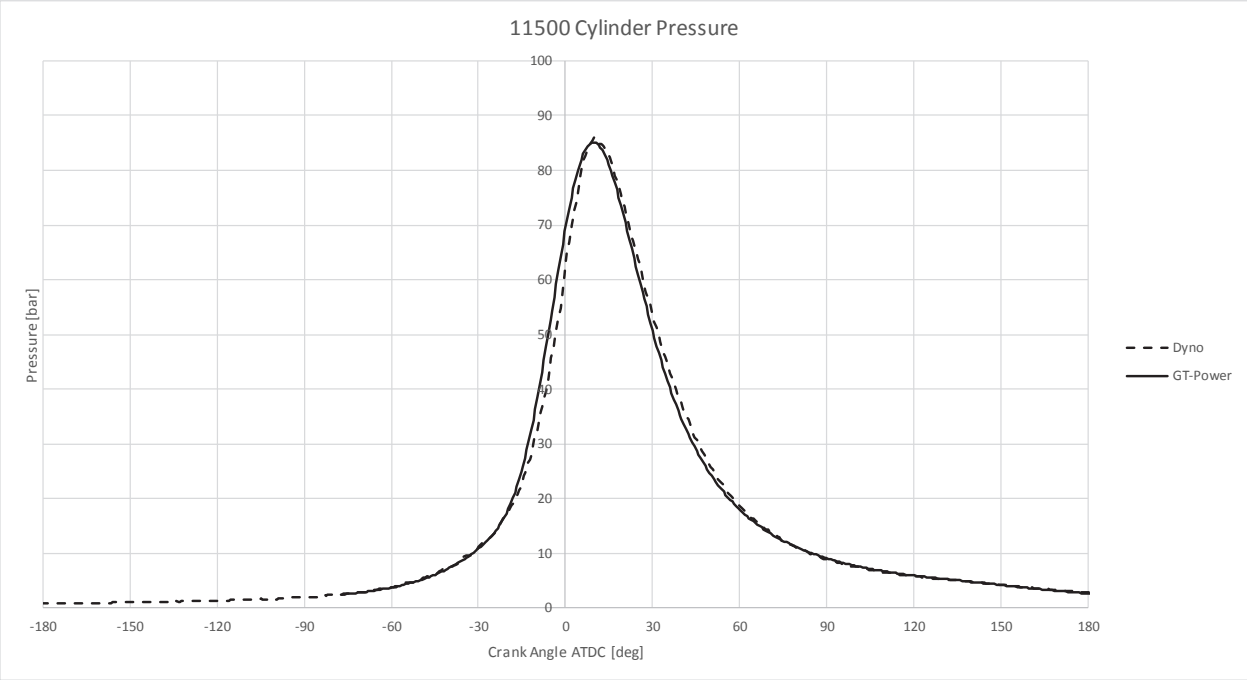

Figure E.1: Cylinder pressure comparison of measured data versus predicted data for 11,500 rpm.

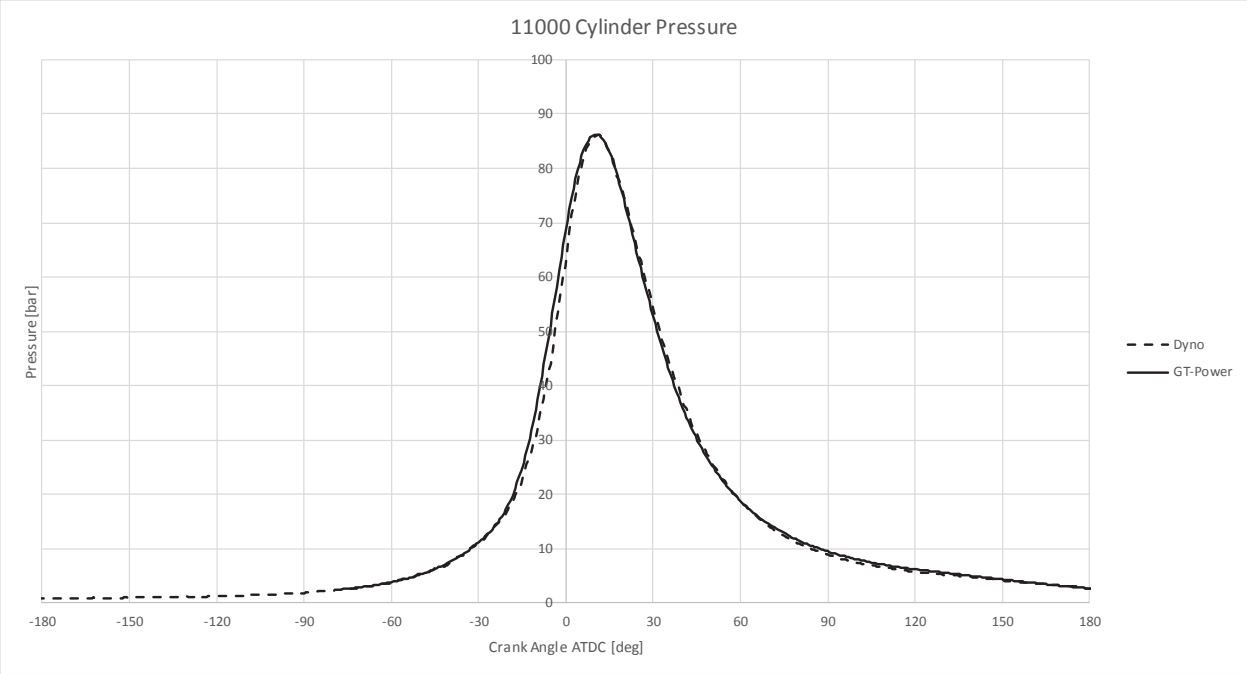

Figure E.2: Cylinder pressure comparison of measured data versus predicted data for 11,000 rpm.

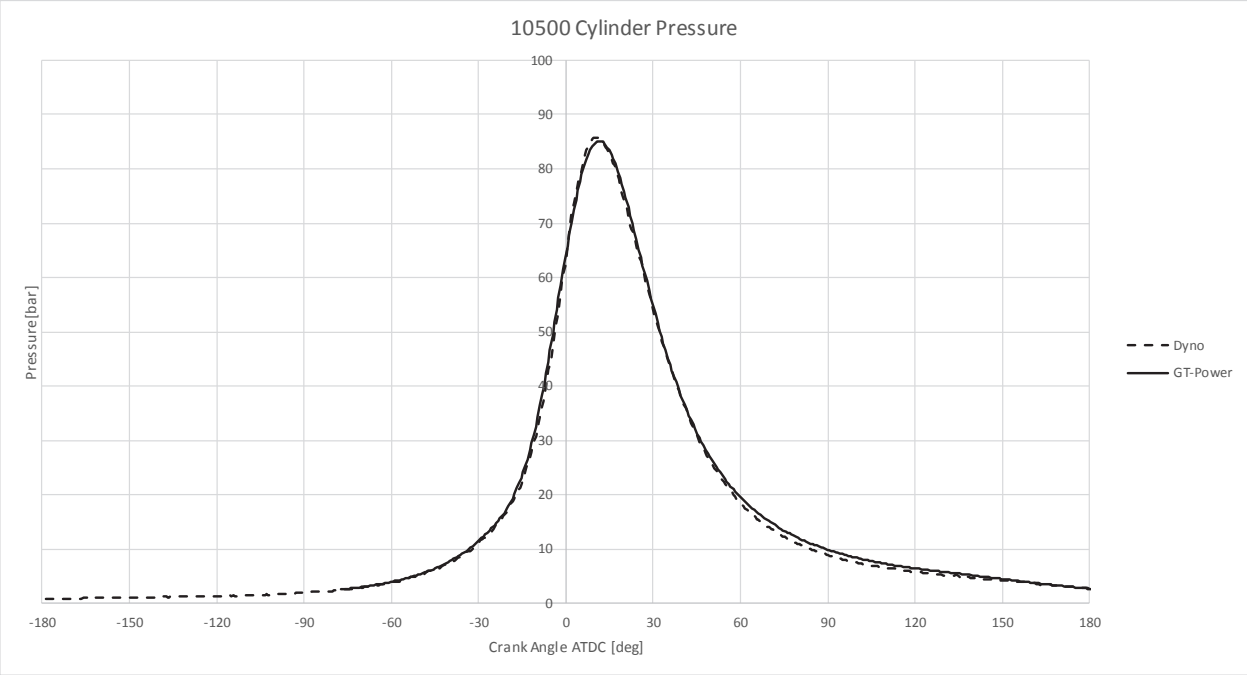

Figure E.3: Cylinder pressure comparison of measured data versus predicted data for 10,500 rpm.

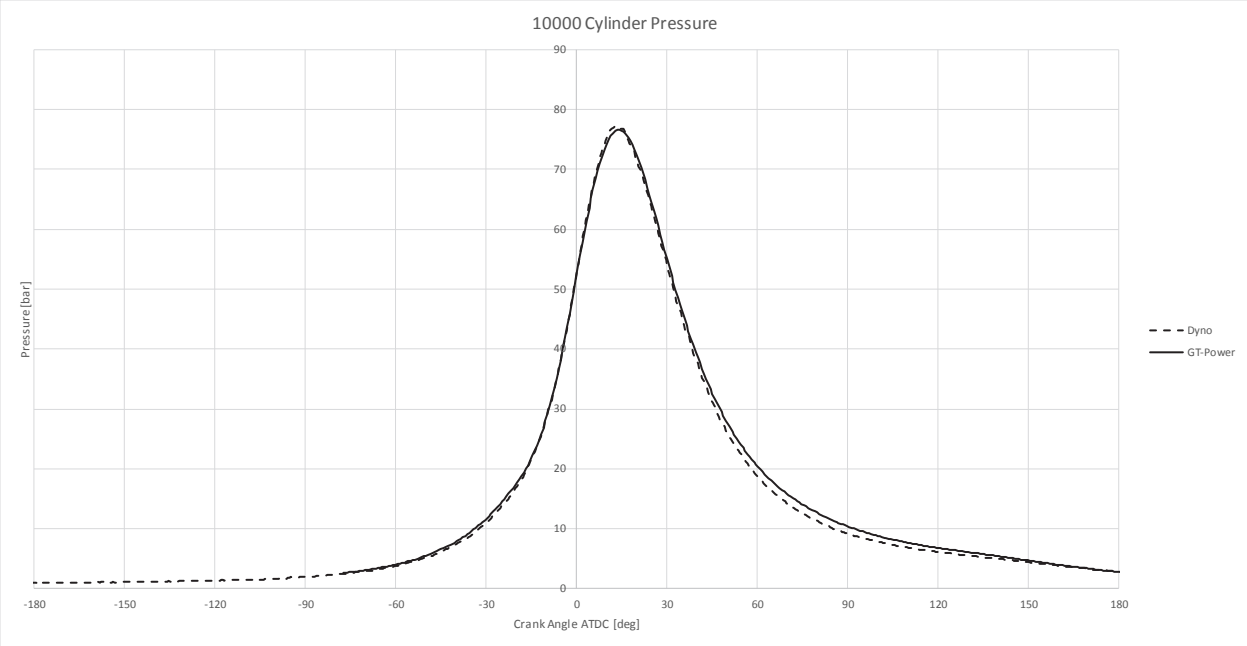

Figure E.4: Cylinder pressure comparison of measured data versus predicted data for 10,000 rpm.

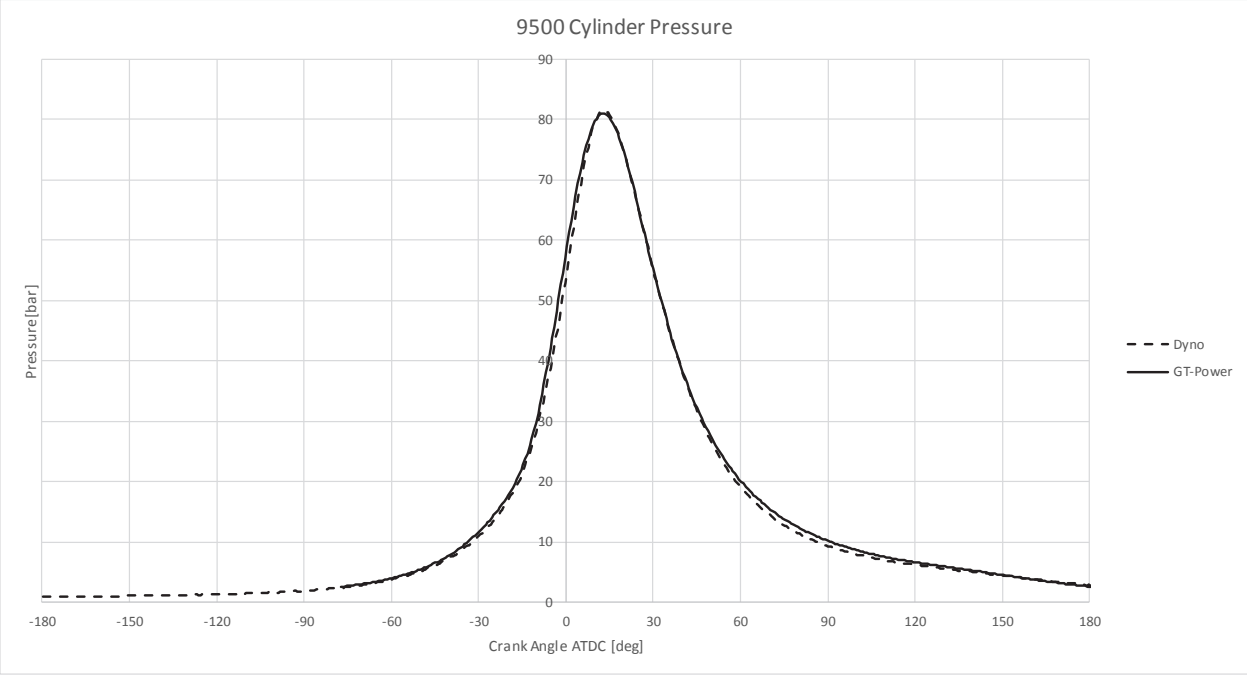

Figure E.5: Cylinder pressure comparison of measured data versus predicted data for 9,500 rpm.

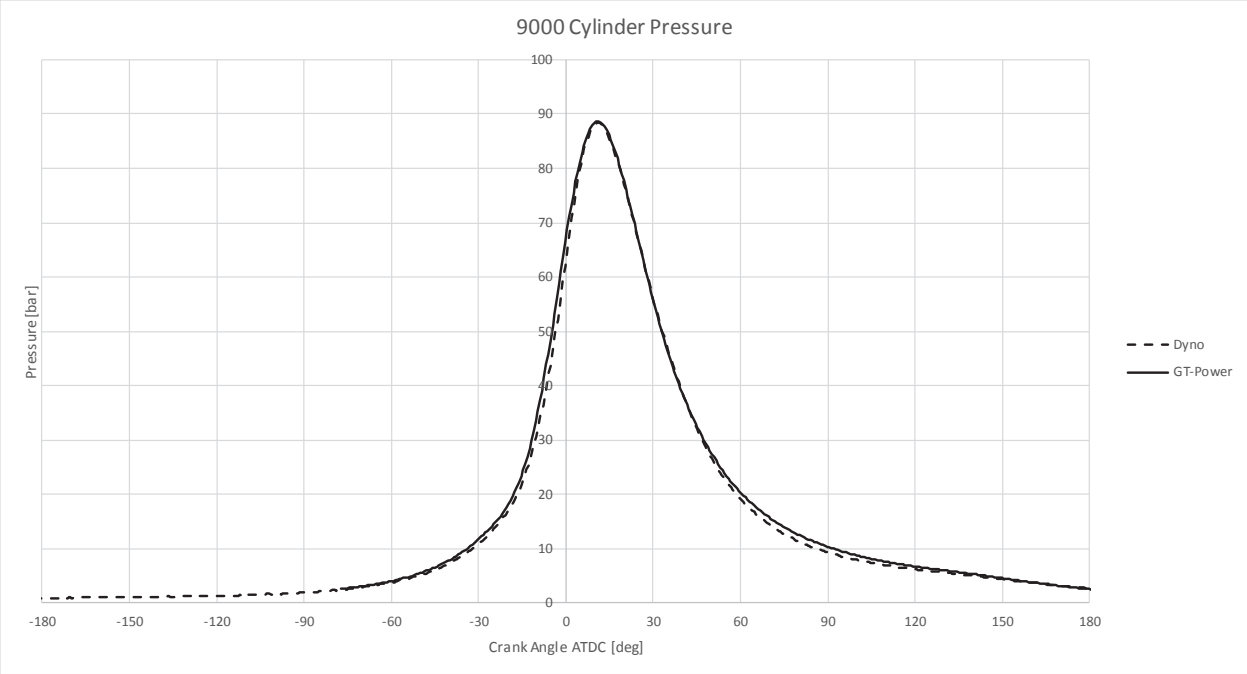

Figure E.6: Cylinder pressure comparison of measured data versus predicted data for 9,000 rpm.

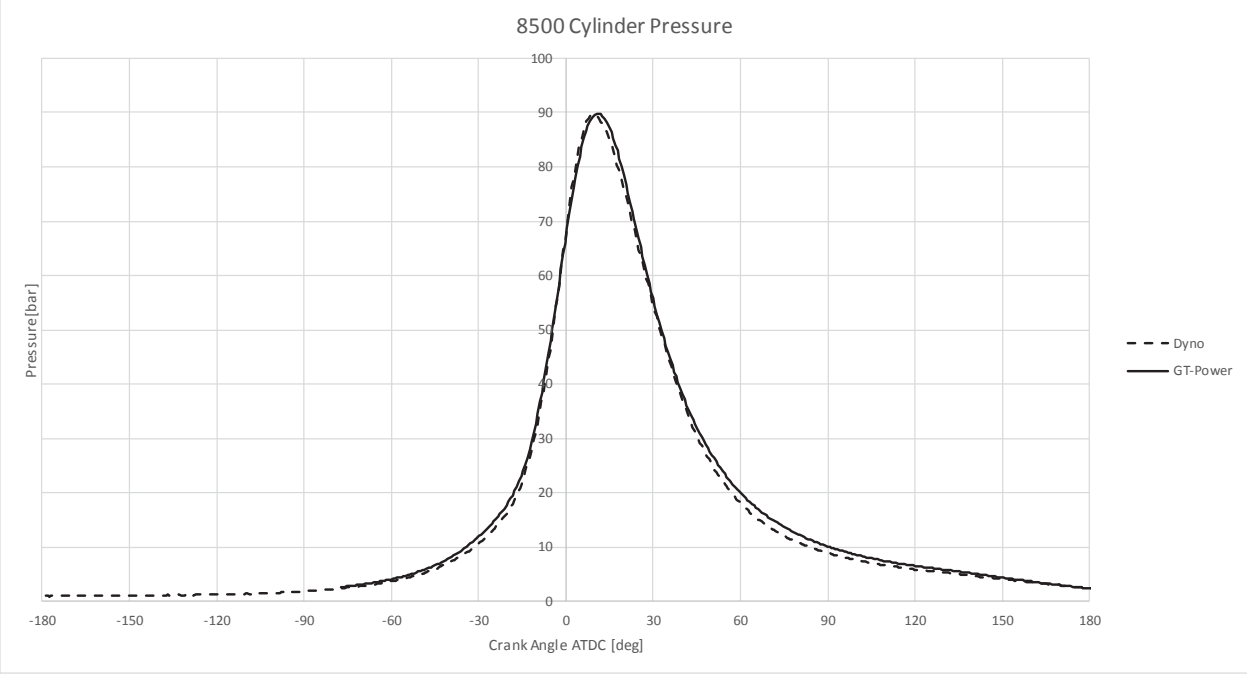

Figure E.7: Cylinder pressure comparison of measured data versus predicted data for 8,500 rpm.

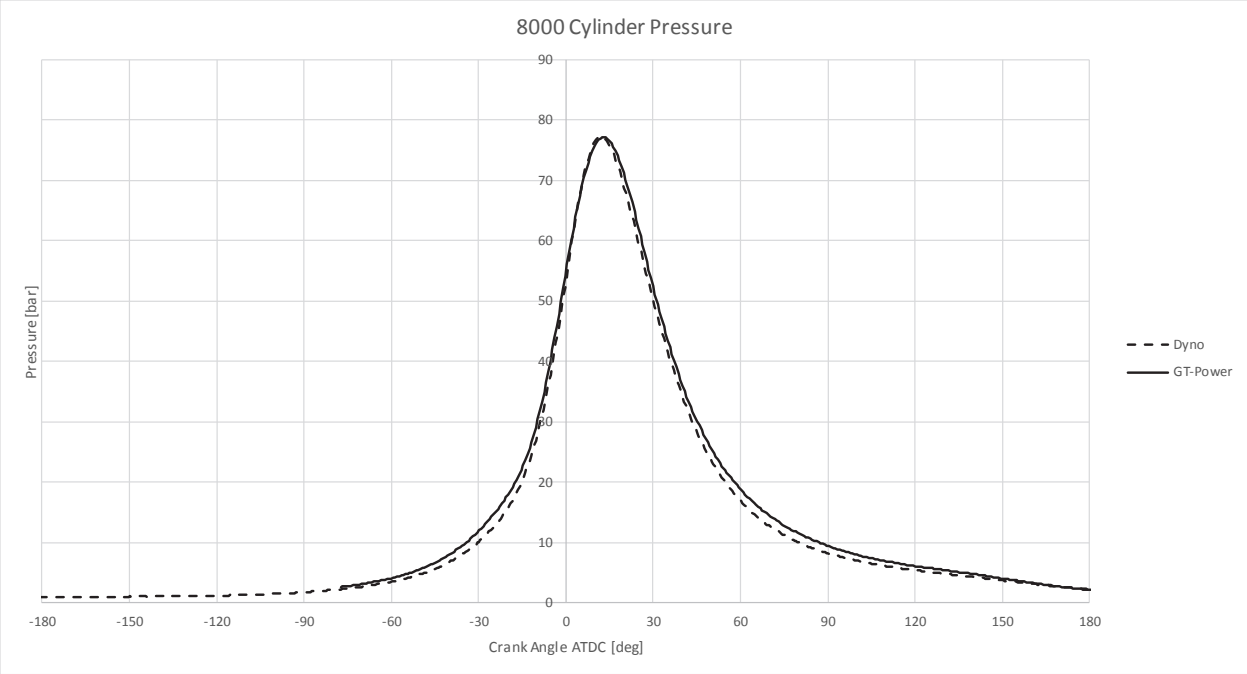

Figure E.8: Cylinder pressure comparison of measured data versus predicted data for 8,000 rpm.

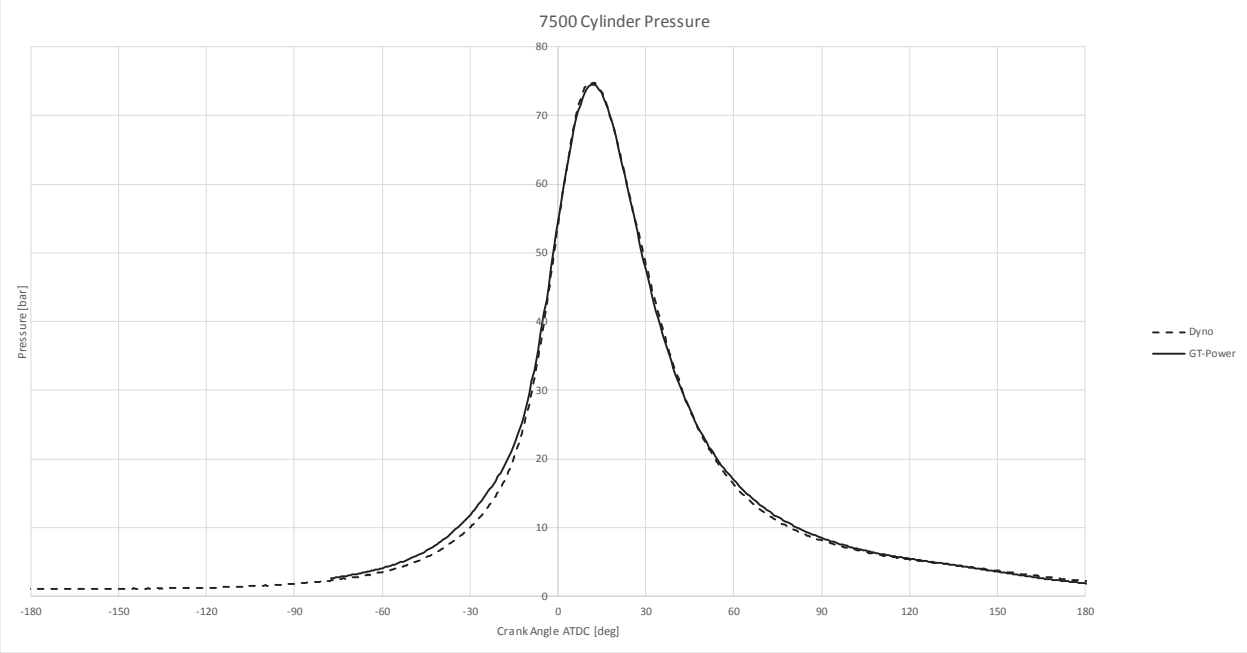

Figure E.9: Cylinder pressure comparison of measured data versus predicted data for 7,500 rpm.

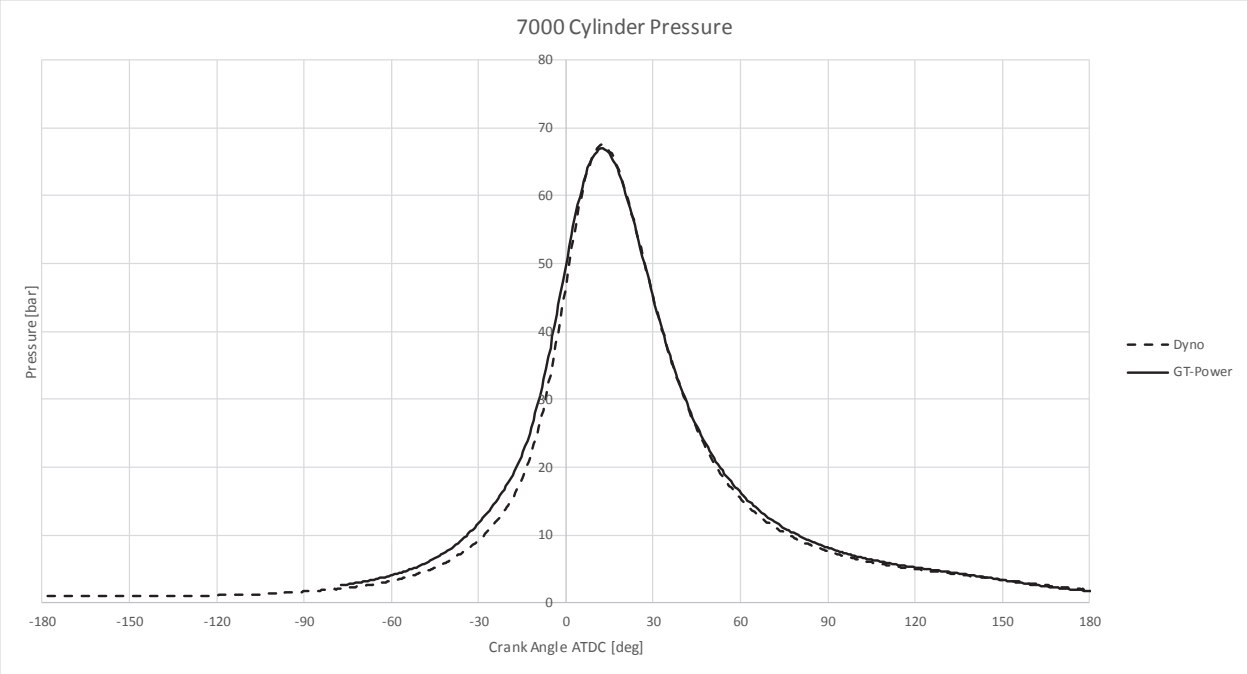

Figure E.10: Cylinder pressure comparison of measured data versus predicted data for 7,000 rpm.

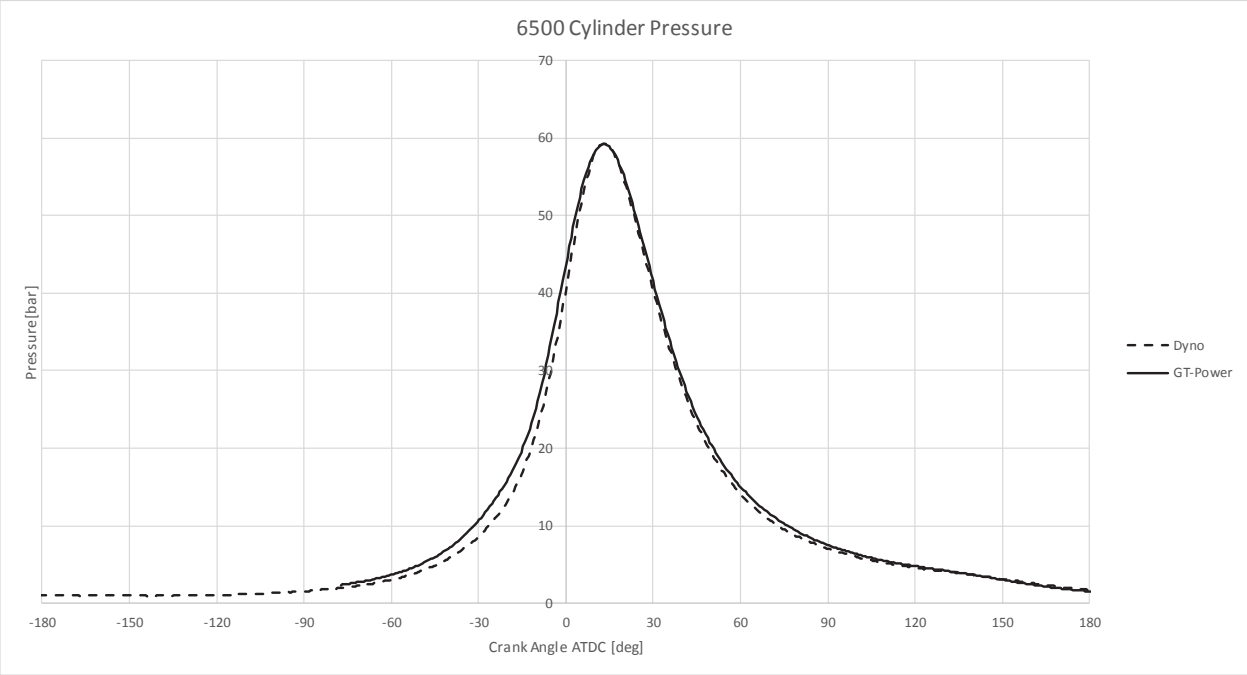

Figure E.11: Cylinder pressure comparison of measured data versus predicted data for 6,500 rpm.

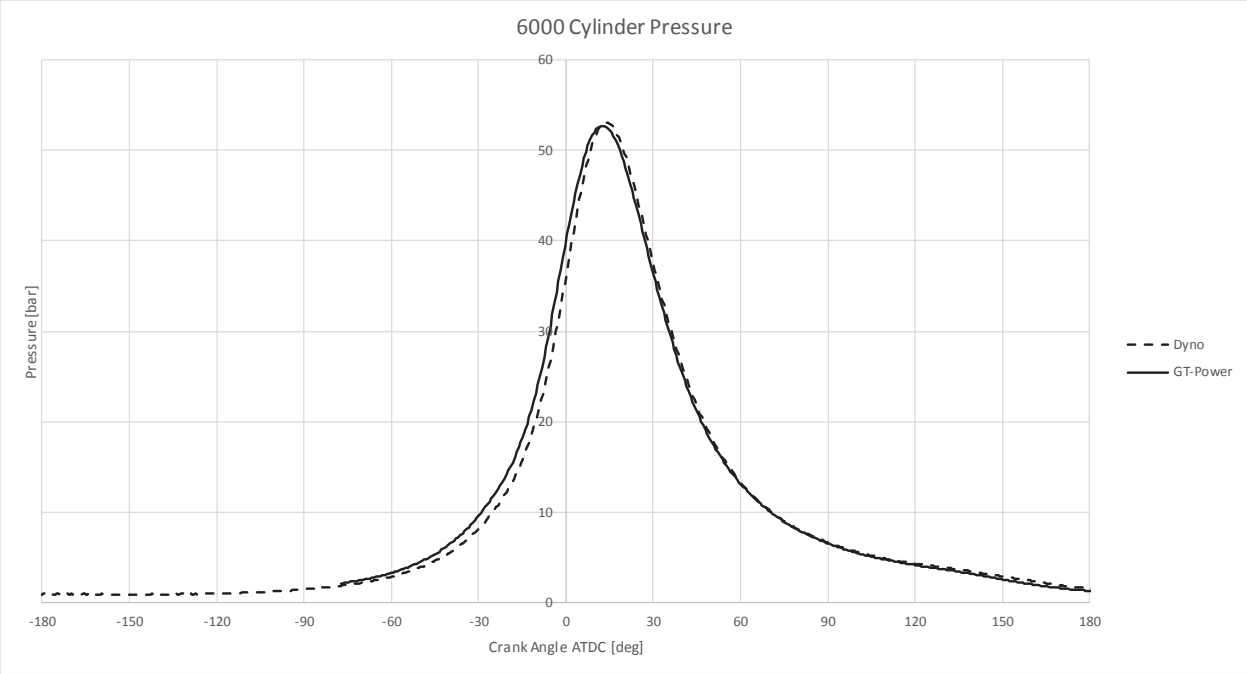

Figure E.12: Cylinder pressure comparison of measured data versus predicted data for 6,000 rpm.

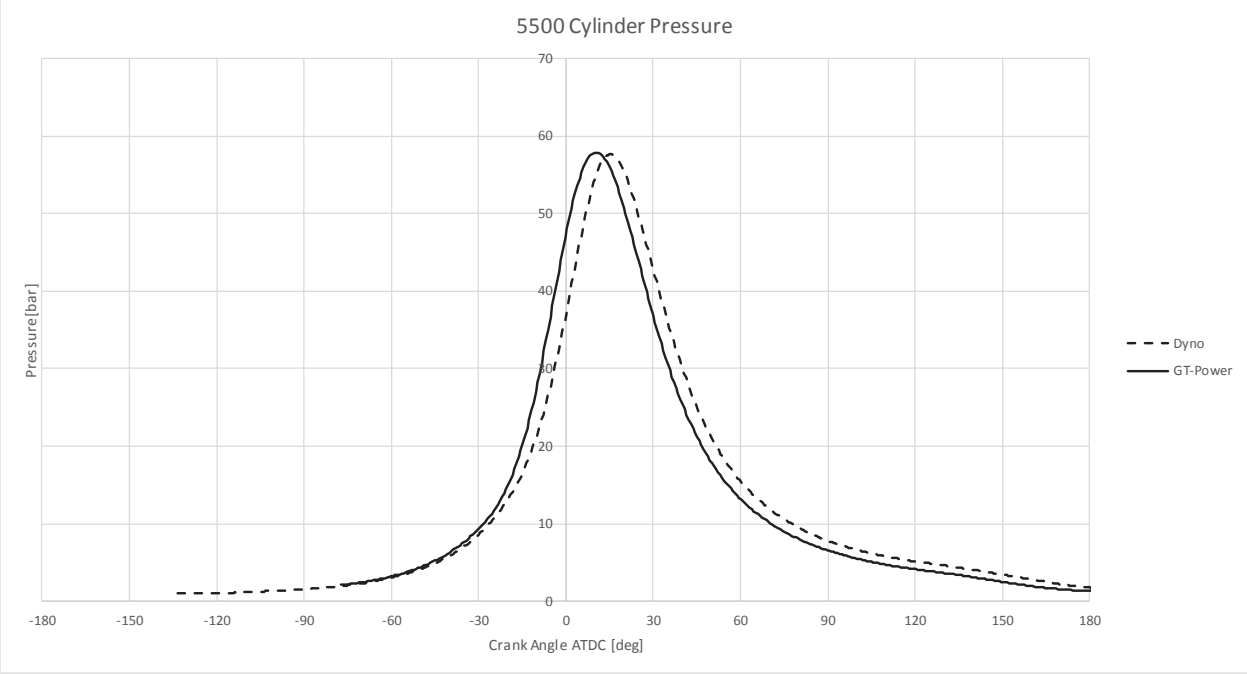

Figure E.13: Cylinder pressure comparison of measured data versus predicted data for 5,500 rpm.

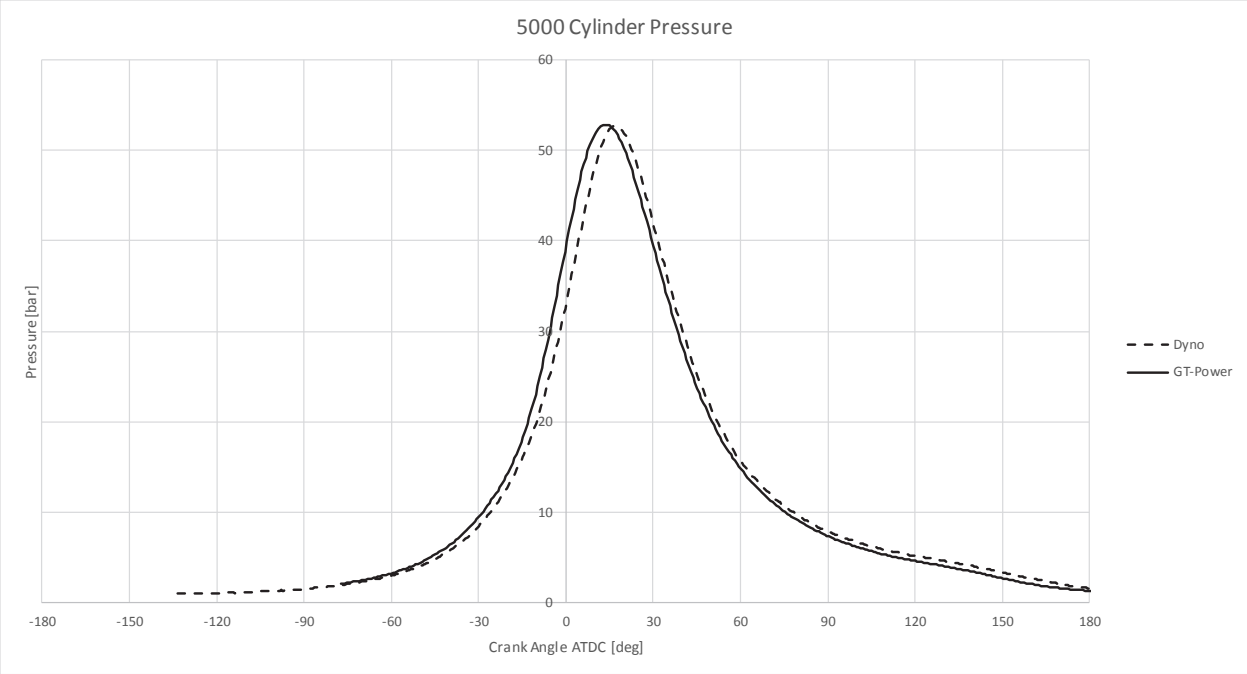

Figure E.14: Cylinder pressure comparison of measured data versus predicted data for 5,000 rpm.